

UCSF

UC San Francisco Electronic Theses and Dissertations

Title

A MicroRNA-21 Surge Facilitates Rapid Cyclin D1 Translation and Cell Cycle Progression in Mouse Liver Regeneration.

Permalink

<https://escholarship.org/uc/item/3n43h9wf>

Author

Ng, Raymond

Publication Date

2012

Peer reviewed|Thesis/dissertation

A microRNA-21 surge facilitates rapid cyclin D1 translation and cell
cycle progression in mouse liver regeneration

by

Raymond Ng

DISSERTATION

Submitted in partial satisfaction of the requirements for the degree of

DOCTOR OF PHILOSOPHY

in

Biomedical Sciences

in the

GRADUATE DIVISION

of the

UNIVERSITY OF CALIFORNIA, SAN FRANCISCO

Dedication

This dissertation is dedicated to my parents Vincent and Evelyn and my girlfriend Wenyu who have supported me during the toughest times during my time at UCSF.

Acknowledgement

The contents of this thesis and my development as a graduate student would not have been possible without the contributions from many people.

First and foremost, I would like to thank the mentorship provided to me by my thesis advisor, Holger Willenbring and my postdoc Guisheng Song. In the last four and a half years, I have learnt a lot from Holger and Guisheng. Holger's optimism and attention to detail combined with Guisheng's practicality and no-nonsense approach allowed me to successfully complete my thesis project. I would like to highlight that Holger's tenacity and drive in this challenging field is incredible. Guisheng played a significant role in providing everyday mentorship, scientific direction and advice.

My thesis committee has been pivotal in shaping this thesis. I am grateful to my committee chair, Andrei Goga, for his inputs and advice. I also like to thank Didier Steiner, an expert in the liver field, for his scientific advice and help with experimental design. His experience working in the liver field has brought enormous value to my thesis.

This thesis will not be possible without my labmates. I thank my wonderful colleagues from the Willenbring lab. They have supported me by offering their scientific inputs, career advice! Once again, I have to thank Guisheng specifically for all the chats about how I should further develop as a scientist and also as an individual. I could not have asked

for better lab members to work with.

Also, a BIG thank you to my fellow colleagues from A*STAR. They are such a bunch of encouraging and enjoyable people to be with. All the informative scientific discussions that we had were extremely useful and interesting and the sharing of reagents and protocols was also a regular occurrence. I would also like to thank all of them who have probably on one or more occasions helped me bring/deliver stuff to and from Singapore! Finally, I would like to say that it's been a great pleasure to have you guys here as friends and colleagues here at UCSF, and I wish all of you good luck with your PhDs!

My parents have always supported me in all the decisions I have made, including pursuing graduate school in overseas institutions. I thank them for their tremendous courage and trust to allow me to pursue an overseas education. I thank them for always asking when I will be back. I would just like to say that I would finally be back home very very soon.

When I first came here, I did not know whether my relationship with Wenyu would work out whilst I was in graduate school. I would like to thank her for her tremendous courage and faith for keeping this long-distance relationship going during the past four and a half years. When everything seems bleak, she would always be there for me. I thank her for all the patience in waiting for my daily phone calls and for all the little presents which she sent from Singapore to cheer me up during the course of my studies. I would also like to thank her for putting up with my lousy temper and

complete lack of consideration at (most if not all) times. Wenyu,I love you and I'm extremely happy that we will be reunited soon.

The genome-wide microRNA microarray screen was conducted by Dr. Amar Deep Sharma and analyzed by Dr. Guisheng Song. The other studies presented in this thesis were performed under the guidance of Dr.Holger Willenbring and Dr. Guisheng Song. My thesis work and its accompanying figures have been accepted for publication in the Journal of Clinical Investigation. The co-authors for the manuscript are Guisheng Song, Garrett R. Roll, Niels Fransden and Holger Willenbring.

A MicroRNA-21 Surge Facilitates Rapid Cyclin D1 Translation and Cell Cycle Progression in Mouse Liver Regeneration.

Raymond Ng

Abstract

MicroRNA-21 (miR-21) has been labeled as an oncomir because it promotes cancer cell proliferation, migration and survival. miR-21 is also expressed in normal cells, however its physiological role is poorly understood. Recently, we found that miR-21 expression is rapidly induced in hepatocytes during liver regeneration after 2/3 partial hepatectomy (2/3 PH). Here, we investigated miR-21's function in regenerating hepatocytes by inhibiting it with an antisense oligonucleotide. To ascertain normal hepatocyte viability and function, we antagonized the miR-21 surge induced by 2/3 PH while preserving baseline expression. We found that knockdown of miR-21 impaired progression of hepatocytes into S phase of the cell cycle mainly through a decrease in cyclin D1 protein but not mRNA. As for the underlying mechanism, we discovered that increased miR-21 expression facilitates cyclin D1 translation in the early phase of liver regeneration by relieving Akt1/mTOR complex 1 signaling and thus eIF-4F-mediated translation initiation from suppression by Rhob. Our findings reveal that miR-21 accelerates cyclin D1 translation in hepatocytes, thereby enabling rapid liver regeneration.

TABLE OF CONTENTS

DEDICATION	III
ACKNOWLEDGEMENT.....	IV
ABSTRACT.....	VIII
LISTOFTABLES	X
LISTOFFIGURES.....	XI
CHAPTER1:INTRODUCTION	1
CHAPTER 2: INDUCED MIR-21 EXPRESSION IS NEEDED FOR CYCLIN D1 TRANSLATION IN THE EARLY PHASE OF LIVER REGENERATION	7
CHAPTER 3: MIR-21 SUPPRESSES RHOB IN THE REGENERATING LIVER	31
CHAPTER 4: MIR-21 PROMOTES CYCLIN D1 TRANSLATION AND CELL CYCLE PROGRESSION IN EARLY LIVER REGENERATION BY SUPPRESSING RHOB AND PROMOTING AKT1-MEDIATED ACTIVATION OF MTORC1.....	39
CHAPTER 5: CONCLUSIONS AND FUTURE DIRECTIONS	50
CHAPTER 6: MATERIALS AND METHODS.....	52
REFERENCES.....	59

List of Tables

Table1:Predicted miR-21 target genes that are negative regulators of the cell cycle.....36

List of Figures

Figure 1 miRNA expression changes in livers of wildtype mice in response to 2/3 PH.....	18
Figure 2 miR-21-ASO injected into the tail vein facilitates inhibition of increased miR-21 expression and de-repression of its target genes after 2/3 PH.....	19
Figure 3 Time course of miR-21 and <i>Ccnd1</i> levels in livers of mice after miR-21-ASO injection or 2/3 PH.....	20
Figure 4 Inhibition of miR-21 decreases cyclin D1 protein but not mRNA in hepatocytes after 2/3 PH.....	21
Figure 5 miR-21 promotes expression of cyclin D1 by facilitating its translation, not by preventing its degradation.....	22
Figure 6 miR-21 regulates cyclin D1 translation.....	23
Figure 7 Inhibition of miR-21 delays S phase entry of hepatocytes after 2/3 PH.....	24
Figure 8 Impaired S phase entry and miR-21 depletion 36 hours after 2/3 PH in hepatocytes of miR-21-ASO-injected mice.....	25
Figure 9 Knockdown of cyclin D1 in hepatocytes during the early phase of liver regeneration impairs S phase entry.....	26
Figure 10 Impaired cyclin D1 translation and cell cycle progression of hepatocytes of miR-21-ASO-injected mice after 2/3 PH are not due to unspecific effects or toxicity caused by the ASO.....	27
Figure 11 Normal mitosis and liver mass restoration despite miR-21 depletion 72 hours after 2/3 PH in hepatocytes of miR-21-ASO-injected mice.....	29
Figure 12 Complete liver mass restoration 192 hours after 2/3 PH in miR-21-ASO-injected mice.....	30
Figure 13 Overexpression of <i>Ccne1</i> , <i>Ccna2</i> and <i>Ccnb1</i> in miR-21-ASO-injected mice.....	31
Figure 14 Moderate suppression of the miR-21 target <i>Pdcd4</i> in early liver regeneration.....	37
Figure 15 Induction of miR-21 in liver regeneration decreases <i>Rheb</i> expression by direct targeting.....	38
Figure 16 miR-21 promotes cyclin D1 translation in liver regeneration by relieving Akt1-mediated activation of mTORC1 from suppression by <i>Rheb</i>	45
Figure 17 Further evidence that miR-21 promotes cyclin D1 translation by relieving Akt1-mediated activation of mTORC1 from suppression by <i>Rheb</i>	47

Figure 18 Overexpression of the miR-21 target PTEN in early liver regeneration.....49

Figure 19 Model of the proposed mechanism of how miR-21 promotes cyclin D1 translation in liver regeneration.....50

Chapter1:Introduction

1.1 Liver Regeneration

The liver is unique in its ability to regenerate itself in response to injury. Hepatocytes and other fully differentiated cells within the adult liver can re-enter the cell cycle and proliferate to generate new tissue to replace the cells lost during injury. Liver regeneration is a very complex and well-orchestrated phenomenon (1). Loss of liver mass can be induced by the administration of different hepatotoxic chemicals such as carbon tetrachloride or 3,5-diethoxycarbonyl-1,4-dihydro-collidine (DDC). These chemicals lead to inflammation, which removes tissue debris, followed by a regenerative response. However, liver regeneration is most commonly studied by performing two-thirds partial hepatectomy (2/3 PH), a surgical procedure which removes two-thirds of the liver mass in rats and mice (2, 3). Since the mouse liver consists of multiple lobes, three of the five lobes (representing 2/3 of the total liver mass) can be removed by an easy surgical procedure without causing any tissue damage to the two remaining lobes (3). The cells, including hepatocytes and cholangiocytes, within the remaining lobes proliferate to restore the liver to its original mass. 2/3 PH has been the method of choice to study liver regeneration due to its reproducibility and the precision of timing of the sequence of ensuing events since all remaining hepatocytes are forced to enter the cell cycle and replicate in order for the organism to survive.

What happens immediately after 2/3 PH is a complex program of responses involving growth factors, cytokines, hormones, extracellular matrix components and other factors. These extracellular mediators activate a carefully orchestrated sequence of intracellular signals resulting in a system-wide coordinated program of gene expression alterations and associated changes in the hepatocytes and other mature cell types in the liver (4). The first cells to enter the cell cycle and undergo DNA synthesis are hepatocytes. All remaining hepatocytes go through a first round of

DNA synthesis, which peaks at 36 hours after 2/3 PH in mice. This restores about 60% of the total hepatocyte mass. A smaller percent of hepatocytes enter into a second round of cell division to establish the original amount of cells. The proliferation of hepatocytes advances from the periportal to pericentral areas of the hepatic lobule as a wave of mitoses with the hepatocytes near the central vein being the last to undergo cell replication (5, 6). Proliferation of biliary epithelial cells occurs slightly later than hepatocytes whilst that of endothelial cells, Kupffer cells and stellate cells starts 48 hours after 2/3 PH. Unlike other forms of organ or tissue regeneration such as skin and small intestine replacement of lost hepatic mass after 2/3 PH does not involve proliferation of stem or progenitor cells. The process of cell proliferation during liver regeneration is complete within 5-7 days after 2/3 PH in mice and 8-15 days in humans.

1.2 Hepatocyte cell cycle entry and progression

In normal adult liver, hepatocytes are highly differentiated and rarely undergo cell division, but they retain the ability to proliferate in response to liver injury. Immediately after 2/3 PH, changes in gene expression occurs within hepatocytes to prime quiescent (G0) hepatocytes to enter the cell cycle (7). This priming phase includes the activation of transcription factors nuclear factor for κ -chain in B cells (NF κ B), signal transducer and activator of transcription-3 (STAT3), activator protein-1 (AP1) and CCAAT enhancer binding protein (C/EBP β) as well as expression of immediate early genes (8). The priming phase is reversible and is neither sufficient to cause DNA replication nor specific for hepatocyte proliferation (8). However, priming is required to make hepatocytes respond fully to at least two different growth factors, hepatocyte growth factor (HGF) and transforming growth factor- α (TGF α), which are highly expressed during liver regeneration (9). HGF is present as an inactive, single-chain molecule bound to the extracellular matrix within the liver. Cleavage by urokinase plasminogen activator (uPA) allows formation of activated HGF heterodimers as early as 30 minutes after 2/3 PH (10, 11). Mitogen-stimulated hepatocytes exit from their quiescent (G0) state and enter G1 phase of the cell cycle. The hepatocytes eventually

encounter a critical checkpoint in mid-late G1 phase, after which they become committed to replication, even if growth factors are withdrawn (12). Passage through this check point in late G1 phase, which is called the restriction point, allows cells to progress through the cell cycle in an autonomous and mitogen-independent manner. Expression of cyclin D1 during liver regeneration is a good marker to indicate when hepatocytes have become autonomous in their replication capacity (13). Progression through the G1 phase is regulated by holoenzyme complexes consisting of D-type cyclins and their cyclin-dependent kinase (Cdk) partners (14-16). In hepatocytes, induction of cyclin D1 protein by extracellular signals appears to be a key intracellular event that regulates passage through G1 phase (14, 17). Overexpression of cyclin D1 increased expression genes implicated in cell cycle progression and DNA replication (18). In addition, transient expression of cyclin D1 in hepatocytes stimulated assembly of active cdk4/cyclin D1 complexes leading to hepatocyte proliferation and liver growth in adult mice(14). These studies suggest that cyclin D1 alone can drive hepatocyte cell cycle progression *in vivo*. Transition through the G1 checkpoint is followed by induction of cyclins E, A and B which regulate progression through late G1, S, G2 and M phases (18).

1.3 Akt/mTOR signaling and translational control

Immediately after 2/3 PH, hepatocytes are primed by numerous cytokines such as tumor necrosis factor- α (TNF α) and interleukin 6 (IL-6) (1, 19-21). This is then followed by growth factor stimulation which leads to hepatocyte cell cycle entry and progression from G1 to S phase (1, 20). Three growth factors of major importance are hepatocyte growth factor (HGF) produced by nonparenchymal cells of the liver, transforming growth factor- α (TGF α) produced by hepatocytes and epidermal growth factor (EGF), the major source of which is the salivary glands in rodents (22). HGF, TGF α and EGF signaling occurs through receptor tyrosine kinases which when activated associate with cytosolic proteins rich in Src homologies such as phosphatidylinositol 3-kinase (PI3K) (1, 22, 23). Activation of PI3K catalyzes the production of phosphatidylinositol-3,4,5-

triphosphate (PIP₃)(24-26).AKT is recruited near to the plasma membrane by PIP₃ and is then phosphorylated at Thr308 by phosphoinositide-dependent kinase 1 (PDK1). In order to fully activate AKT, it is subsequently phosphorylated at Ser473 (27, 28). Activated AKT translocates to the nucleus and activates mTOR and downstream targets.The PI3K/Akt pathway has been shown to be dysregulated in many forms of cancers and strongly promotes cell proliferation, growth, survival and protein synthesis by activation of multiple downstream pathways and transcription factors(29, 30).Phosphorylation of Akt leads to the subsequent phosphorylation of downstream targets such as mammalian target of rapamycin (mTOR), eventually affecting cell growth and survival (31). mTOR has emerged as a major effector of cell growth and proliferation via the regulation of protein synthesis, in particular protein translation, through a large number of downstream targets (32, 33). Some of these targets are directly phosphorylated by mTOR. In response to mitogen stimulation, mTOR regulates translation initiation through 2 distinct pathways: (1) phosphorylation and activation of ribosomal p70 S6 kinase (S6K1), and (2) cap-dependent translation via eukaryotic initiation factor 4E (eIF4E), which binds the 7me GpppN cap of mRNA and directs the correct positioning of ribosomal subunits to initiate translation (32, 33). In the case of eIF4E, mTOR directly phosphorylates the eIF4E binding protein (4E-BP1),which acts as a repressor of eIF4E, causing it to dissociate from eIF4E. eIF4E is then free to bind to eIF4G thereby promoting the assembly of the eIF4F initiation complex (32). Two oncogenes cyclin D1 and Myc are targets of eIF4E-mediated cap-dependent translation and thus regulated by mTOR. These results suggest that the Akt/mTOR pathway, which is activated after 2/3 PH,may control hepatocyte cell cycle progression through S6K1 and 4E-BP1/eIF4E (32, 34).

1.4 microRNA biogenesis and microRNA-21

microRNAs (miRNAs) are a class of naturally occurring small non-coding RNAs (approximately 20-23 nucleotides long) that target protein-coding mRNAs by repressing translation or causing mRNA degradation (35, 36). miRNA genes are transcribed by either RNA polymerase II or III into

primary miRNA transcripts (37-39). The primary miRNAs are then trimmed into hairpin intermediates (pre-miRNAs) by the microprocessor complex consisting of RNase III Drosha and DiGeorge syndrome critical region gene 8 (DGCR8) (40). The pre-miRNAs, which have a stem-loop structure, are then exported out of the nucleus into the cytoplasm after being recognized by the nuclear export factor exportin-5 (41-43). Following export, the cytoplasmic endonuclease Dicer cleaves the pre-miRNA stemloop to produce miRNA duplexes. The duplex strand is separated and one strand is selectively incorporated into the RNA-induced silencing complex (RISC) to function as a guide molecule in translational control or mRNA cleavage. Although miRNAs operate in a similar fashion as short interfering RNAs (siRNAs), they typically target a cluster of genes instead of one specific gene. It has been predicted that an average miRNA can have more than 100 targets (44). In mammals, miRNAs are predicted to control the activity of approximately 50% of all protein-coding genes. Functional studies indicate that miRNAs participate in the regulation of almost every cellular process investigated so far and that changes in their expression are associated with many human pathologies (45). However, it has become increasingly clear that not all miRNAs are equally important; diverse high-throughput screenings of various systems have identified a small number of key functional miRNAs repeatedly (46). Evidence is rapidly accumulating for a prominent role of microRNA-21 (miR-21) in cancer. Since its identification as the miRNA most commonly and strongly upregulated in the human brain tumor glioblastoma (47), miR-21 has been further shown to be overexpressed in almost all types of cancer and has been shown to promote cancer cell proliferation, migration and survival (46, 48-50). The mature miR-21 is perfectly conserved in mammals and is encoded by a single gene. The human miR-21 gene is mapped to chromosome 17q23.2 where it overlaps with the protein-coding gene vacuole membrane protein (VMP1) (38, 51). Several primary transcripts of miR-21 (pri-miR-21) have been identified in a number of different cell types including a 3.5kb and 4.3 kb transcript which were detected due to the presence of different miR-21 promoters (38, 51). Bioinformatic and functional analysis of the consensus sequences within the miR-21 promoter region identified activation protein 1 (AP-1) and signal transducer and activator of transcription 3 (STAT3) as transcription factors which can bind

to the miR-21 promoter and enhance its transcriptional activation (51, 52). miR-21 has also been shown to negatively regulate tumor suppressor genes such as PTEN, programmed cell death 4 (PDCD4) as well as BTG2 further cementing its role as an oncomiR (53-55). Since a single miRNA can regulate multiple target genes, the question remains what other target genes does miR-21 suppress and if the identified mechanisms are conserved during normal cell proliferation and migration occurring during development.

Chapter 2: Induced miR-21 expression is needed for cyclin D1 translation in the early phase of liver regeneration

2.1 Introduction

Many genes are differentially expressed immediately after 2/3 PH, during the immediate early response phase (1, 7, 8, 20). Many of these genes have been identified by performing microarrays or high throughput RNA sequencing that can measure the expression of entire transcriptomes of hepatocytes. In order to determine which of these genes play a crucial role in hepatocyte proliferation, scientists have made use of transgenic mice in which the gene of interest was deleted or overexpressed. Such studies were successful in contributing new knowledge about the early phases of liver regeneration (8). However, even though miRNAs have been shown to regulate almost every cellular process in the organism (45), their functions during liver regeneration has not been thoroughly examined. Recently, we showed that hepatocyte-specific loss of miRNAs leads to a delay in G₁ to S phase progression during liver regeneration suggesting that miRNAs may play a role in regulating cell proliferation during liver regeneration (56). Hepatocytes of mice with inactivated DGCR8 were miRNA-deficient and exhibited a delay in cell cycle progression involving the G₁ to S phase transition(55). We and others also found that the expression of miR-21 is induced during the early phase of liver regeneration in mice (55, 57) and rats (58). This rapid surge in miR-21 expression during the first 18 hours of liver regeneration corresponds to the time during which hepatocytes exit G₀ phase and enter the cell cycle suggesting that this surge in miR-21 and a corresponding decline in target gene expression may promote hepatocyte cell cycle entry and G₁ to S phase transition.

Because miR-21 expression levels are high in the quiescent hepatocytes of the normal liver (55), we reasoned that complete miR-21 depletion by genetic deletion may disturb normal hepatocyte physiology, which may confound analyses of miR-21's role in cell cycle regulation. However, the

advent of chemically modified antisense oligonucleotides (ASOs), especially those containing locked nucleic acids (LNAs), allows for dose-dependent, temporally controlled specific inhibition of endogenous miRNAs because LNAs exhibit high binding affinity to complementary RNA target molecules by forming stable heteroduplexes with mature miRNAs and high stability *in vivo*(59).Therefore, we took an alternative approach and antagonized specifically the miR-21 surge induced by 2/3 PH in hepatocytes with a miR-21 antisense oligonucleotide (miR-21-ASO). This approach allowed us to antagonize the increase in miR-21 expression whilst keeping miR-21 expression at physiological levels and also to temporally regulate miR-21 expression levels. Thus, in this study, the unique ability of ASOs to specifically suppress miRNA expression in cells or tissues was exploited to study miR-21's function during early liver regeneration (60, 61).

2.2 Results

*Global miRNA deficiency in hepatocytes impairs G1 to S phase progression of hepatocytes after 2/3 PH.*To identify miRNAs regulating hepatocyte S phase entry during liver regeneration, analysis of global miRNA expression was performed during the first 36 hours after 2/3 PH in wildtype mice. Pilot analyses allowed further studies to focus on miRNA expression changes during the first 18 hours after 2/3 PH. Previous studies showed that many genes are differentially expressed after 2/3 PH. However, when a stringent cut-off of $P < 0.001$ was used, only 7 of ~430 mouse miRNAs analyzed were found to have significantly altered expression after 2/3 PH (Fig. 1A). Intriguingly, miR-21, a known promoter of proliferation in cancer,(46) was most significantly induced. miR-21 peaked at 18 hours after 2/3 PH, that is after hepatocytes transitioned from G0 into G1 but before they passed the restriction point and entered S phase (Fig. 1B). Recent studies showed that miR-21 is transcriptionally regulated by AP-1(51) and STAT3(52),proteins activated early in liver regeneration(1). Since both sets of findings fit well with a lack of miR-21 impairing the transition of regenerating hepatocytes from G1 to S phase, further analyses were focused on miR-21.

miR-21-ASO is effective in timed and dosed antagonism of miR-21 in the regenerating liver. 2/3 PH in mice caused increased miR-21 expression that was detectable at 6 hours, peaked between 18 and 24 hours, and returned to almost normal levels by 36 hours after the surgery (Figure 2A). The timing of the miR-21 surge suggests that it plays a role in the regulation of cell cycle events preceding S phase, a hypothesis that is indirectly supported by our previous finding of delayed S phase entry after 2/3 PH in hepatocytes lacking all miRNAs(55).

To determine whether and how miR-21 contributes to regulation of the early phase of liver regeneration, 2/3 PH would have to be performed in mice incapable of increased miR-21 expression in hepatocytes. Fully depleting miR-21 could prohibit unbiased analysis of miR-21's effect on hepatocyte proliferation because miR-21 is expressed at high levels in quiescent hepatocytes and little is known about its role in cellular homeostasis (55). Thus, the experiment was designed to antagonize the miR-21 surge occurring in the liver after 2/3 PH while maintaining physiological miR-21 expression levels.

For this purpose, a miR-21-ASO stabilized with LNAs similar to a miR-122-ASO that was recently reported to efficiently inhibit this highly abundant miRNA in hepatocytes in vivo was generated (61, 62). To establish timed and dosed miR-21 inhibition in vivo, we determined the onset, extent and duration of changes in liver miR-21 expression after tail vein injection of the miR-21-ASO. We found that a single dose of 25 µg/g body weight miR-21-ASO decreases liver miR-21 levels 4-fold by 6 hours after injection, and that the suppression of miR-21 increases with time and lasts for at least 36 hours (Figure 3A).

Knowing that miR-21-ASO inhibits miR-21 in the liver rapidly and progressively, we decided to inject it after 2/3 PH to antagonize the surge in miR-21 expression, but avoid complete knockdown of miR-21 during the early phase of liver regeneration. We aimed at suppressing miR-21 to uninduced levels at

18 hours after 2/3 PH, that is, at the peak of the rapid surge in miR-21 expression (Figure 2A). We reasoned that, due to increased portal vein flow, uptake of intravenously injected miR-21-ASO into hepatocytes after 2/3 PH could be even more efficient than into hepatocytes in the normal liver. Therefore, we used a single dose of 25 $\mu\text{g/g}$ body weight miR-21-ASO as in normal mice, but tested 2 injection time points, 6 and 10 hours after 2/3 PH (Figure 1A). However, we found that the levels of liver miR-21 suppression at 18 hours after 2/3 PH were indistinguishable between the 2 time points (Figure 2B). Residual miR-21 levels in livers of these mice were within 50% of that of control mice (injected with the carrier NaCl 0.9%), which resulted in normal liver function tests (data not shown). Considering that miR-21 is induced approximately 2-fold after 2/3 PH, this finding suggests an almost linear relationship between miR-21-ASO dose and miR-21 suppression in both regenerating and normal liver (Figure 2B and Figure 1A). Importantly, we found that mRNA levels of B-cell translocation gene 2 (*Btg2*), a known miR-21 target gene that is normally repressed at 18 hours after 2/3 PH (55), were de-repressed in mice injected at either of the 2 time points (Figure 2C). These results establish that miR-21-ASO can be used to specifically antagonize the increased expression of miR-21 and its downstream effects in the regenerating liver.

Induced miR-21 expression is needed for cyclin D1 translation in the early phase of liver regeneration.

Next, we analyzed the livers of the mice injected with miR-21-ASO for expression of cell cycle phase-specific markers by immunostaining (Figure 4, A and B). One of the earliest cell cycle events after 2/3 PH is induction of cyclin D1 expression by extracellular mitogenic signals (1, 7). Cyclin D1 controls transition of hepatocytes through checkpoints in G1 phase. Subsequent sequential activation of cyclins E1, A2 and B1 allows hepatocytes to progress into late G1, S, G2 and M phase. As expected, many hepatocytes in control mice expressed cyclin D1, indicating that they were progressing through G1 phase at 18 hours after 2/3 PH. A small subset of the cells was already in late G1 or S phase, as evident from positive Ki67 or proliferating cell nuclear antigen (PCNA) staining, respectively. In contrast, cyclin D1, Ki67 and PCNA expression was rarely or not detectable in hepatocytes of mice injected

with miR-21-ASO at 6 hours after 2/3 PH. This finding suggests that cyclin D1 expression and G1 phase transition of hepatocytes after 2/3 PH depend on induced miR-21 expression.

However, when we analyzed the mice injected with miR-21-ASO at 10 hours after 2/3 PH, we found that their hepatocytes stained normally for all 3 cell cycle markers (Figure 4, A and B). This finding was surprising because miR-21 levels were indistinguishable between livers of mice injected with miR-21-ASO at 10 versus 6 hours after 2/3 PH (Figure 2B). Considering that miR-21-ASO de-represses miR-21 target genes in hepatocytes by 8 hours after tail vein injection (Figure 2C), this finding reveals that the miR-21 surge promotes the expression of cyclin D1 before and around 14 hours, but is not needed anymore around 18 hours after 2/3 PH.

To confirm the discrepancy in cyclin D1 expression between mice injected with miR-21-ASO at 6 versus 10 hours after 2/3 PH, we analyzed their livers using immunoblotting and qRT-PCR. In control mice, the induction of *Ccnd1* mRNA after 2/3 PH mirrored that of miR-21 and *Ccnd1* mRNA was rapidly translated into protein (Figure 2B, Figure 3A and Figure 4C). After treatment with miR-21-ASO, cyclin D1 protein levels were normal in mice injected at 10 hours after 2/3 PH but low in mice injected at 6 hours after 2/3 PH (Figure 4C). *Ccnd1* mRNA levels, however, were identical in livers of mice injected at the 2 time points (Figure 4D). The uncoupling of *Ccnd1* mRNA and protein levels in mice injected with miR-21-ASO at 6 hours after 2/3 PH indicated that miR-21 either promotes the translation or prevents the degradation of cyclin D1.

The activity of the enzyme mainly responsible for degradation of cyclin D1, glycogen synthase kinase 3 beta (Gsk3b), is inhibited by phosphorylation (63). Because Gsk3b was expressed normally and did not show inhibitory phosphorylation in miR-21-ASO-injected mice at 18 hours after 2/3 PH (Figure 5A), we reasoned that the effect of miR-21 on cyclin D1 expression is due to promotion of translation.

To test this hypothesis, we determined whether cyclin D1 translation is miR-21-dependent. First, we investigated whether altering the levels of miR-21 in Hepa1,6 mouse hepatoma cells affects cyclin D1 protein levels. For this purpose, we transfected the cells with miR-21-ASO or miR-21 mimic (Figure 6A and Figure 5, B and C). We found that inhibiting miR-21 decreased cyclin D1 protein levels whereas adding miR-21 increased them. Next, we performed polysome analysis to determine whether miR-21 acts on cyclin D1 translation (64). We fractionated cytoplasmic lysates from Hepa1,6 cells transfected with miR-21-ASO and control cells by sucrose density gradient centrifugation and distinguished fractions containing no ribosomes (untranslated fractions), single ribosomes (monosomal fractions) or multiple associated ribosomes (polysomal fractions) (Figure 5D and Figure 6B). Using qRT-PCR, we found that overall *Ccnd1* mRNA levels in unfractionated RNA of Hepa1,6 cells were not altered by miR-21-ASO transfection (Figure 5E), which was in accordance with our findings in vivo (Figure 4D). However, *Ccnd1* mRNA levels were decreased in RNA isolated from polysomal fractions of miR-21-depleted Hepa1,6 cells, which are most actively translated (Figure 6C). Viewed together, our results show that the miR-21 surge induced by 2/3 PH functions to facilitate translation of cyclin D1 in the early phase of liver regeneration.

Hepatocyte entry into S phase after 2/3 PH is delayed when promotion of cyclin D1 translation by miR-21 is absent. Considering that cyclin D1 initiates the cyclin activation cascade after 2/3 PH (1, 7), we next asked whether impaired cyclin D1 translation due to miR-21 inhibition limits the ability of hepatocytes to progress beyond the restriction point in late G1 and enter S phase. As expected, many hepatocytes in control mice continued to express cyclin D1 at 36 hours after 2/3 PH (Figure 7, A and B). Staining for Ki67 and PCNA both showed a large number of positive hepatocytes, indicating that many hepatocytes had not only progressed to late G1 but had already entered S phase in these mice. In contrast, Ki67 and PCNA staining showed significantly fewer hepatocytes in S phase in mice injected with miR-21-ASO at 6 hours after 2/3 PH than in control mice (Figure 7, A and B), which we confirmed by 5-bromo-2-deoxyuridine (BrdU) labeling (Figure 8, A-D).

In accordance with our findings at 18 hours after 2/3 PH, cyclin D1 protein levels were lower in miR-21-ASO-injected mice than in control mice (Figure 7C and Figure 4C). *Ccnd1* mRNA levels remained equal (Figure 7D and Figure 4D), which showed that cyclin D1 translation was still impaired. To ascertain that decreased cyclin D1 levels were responsible for impaired S phase entry of hepatocytes in miR-21-ASO-injected mice after 2/3 PH, we directly inhibited cyclin D1 with a *Ccnd1*-ASO. Tail vein injection of *Ccnd1*-ASO at 6 hours after 2/3 PH markedly blunted the increase in cyclin D1 mRNA and protein levels normally observed at 36 hours after 2/3 PH (Figure 9, A and B). Quantification of BrdU-labeled hepatocytes in *Ccnd1*-ASO-injected mice revealed that cyclin D1 deficiency impaired S phase entry to a similar degree as miR-21 deficiency (Figure 9, C and D). The result suggests that miR-21 acts mainly through cyclin D1 to promote hepatocyte proliferation in the early phase of liver regeneration.

To further ascertain that the hepatocyte cell cycle defect observed in miR-21-ASO-injected mice is due to miR-21 deficiency, and not toxicity caused by the ASO, we generated miR-21-MM-ASO, a control ASO that differs from miR-21-ASO in 4 mismatched base pairs. As was done with miR-21-ASO, we injected miR-21-MM-ASO into the tail vein of mice at 6 hours after 2/3 PH and analyzed their livers at 18 or 36 hours after the surgery. As expected, we found that the modification prohibited miR-21-MM-ASO from binding and inhibiting miR-21, as was evident from unaltered levels of miR-21 and its target genes (Figure 10A). Furthermore, injection of miR-21-MM-ASO did not alter cyclin D1 protein levels or hepatocyte cell cycle entry and progression during liver regeneration (Figure 10, B-F). These results rule out miR-21-unrelated effects as the cause of impaired cyclin D1 translation and cell cycle progression in hepatocytes of mice injected with miR-21-ASO.

Interestingly, we noted that the difference in liver cyclin D1 protein levels between controls and miR-21-ASO-injected mice grew smaller with time after 2/3 PH (Figure 7C and Figure 4C), indicating that cyclin D1 translation was improving. Because miR-21 was still repressed and its target genes de-repressed (Figure 8, C and D), the finding suggested that increased miR-21 levels were no longer essential for translation of cyclin D1 at 36 hours after 2/3 PH. To investigate the possibility that impaired S phase entry was eventually compensated for in miR-21-ASO-injected mice, we analyzed mice at later time points after 2/3 PH. We found that the number of BrdU-labeled hepatocytes was similar between miR-21-ASO-injected and control mice at 72 hours after 2/3 PH (Figure 11, A and B). Moreover, both groups showed the same number of hepatocytes staining positive for phosphorylated histone H3 (pH3), a marker of mitosis (Figure 11, A and C). In miR-21-ASO-injected mice, miR-21 continued to be inhibited, although its levels had increased 2-fold compared to 36 hours after 2/3 PH (Figure 11D). These findings indicated that miR-21-depleted hepatocytes had overcome the G1 phase arrest and transitioned through S and into M phase. Moreover, normal levels of mitosis at 72 hours after 2/3 PH suggested that hepatocytes in miR-21-ASO-injected mice had compensated for the delay in S phase entry. This interpretation was supported by the finding that the extent of liver mass restoration was similar between miR-21-ASO-injected and control mice at this time point (Figure 11E). Indeed, at 192 hours after 2/3 PH, when normal liver regeneration is complete, miR-21-ASO-injected mice had the same ratio of liver to body weight as control mice (Figure 12A). In addition, hepatocytes in miR-21-ASO-injected mice had returned to normal quiescence and expressed almost normal levels of miR-21 by that time (Figure 12, B-D).

In findings similar to ours, a previous study reported delayed, but not permanently blocked, S phase entry in *Ccnd1*^{-/-} mice after hepatomitogen application (65). The study suggested that overexpression of cyclin E can compensate for the lack of cyclin D1 and facilitate cell cycle progression. Thus, we decided to determine the expression levels of cyclins downstream of cyclin D1 in livers of miR-21-ASO-injected mice after 2/3 PH. We found that *Ccne1* was 8-fold higher in miR-21-ASO-injected mice than in control mice at 18 hours after 2/3 PH and continued to be overexpressed until 72 hours

(Figure 13A). *Ccna2* and *Ccnb1* were also overexpressed in miR-21-ASO-injected mice, most likely as a consequence of *Ccne1* overexpression (Figure 13, B and C). These results suggest that cyclin E1 overexpression, potentially aided by emerging translation of cyclin D1, can overcome the G1 phase arrest in miR-21-depleted hepatocytes.

2.3 Discussion

Previously, we and others observed a surge in miR-21 expression in G1 phase in hepatocytes after 2/3 PH (55, 66, 67). Here, we investigated the function of induced miR-21 expression in liver regeneration by specifically antagonizing the miR-21 surge, but not baseline miR-21 expression, with miR-21-ASO, a short LNA-stabilized antisense oligonucleotide inhibitor of miR-21. This partial knockdown strategy revealed that increased miR-21 expression facilitates cyclin D1 translation in early liver regeneration.

Our results further show that promotion of cyclin D1 translation by miR-21 is important for rapid G1 phase progression and S phase entry of hepatocytes after 2/3 PH. In mice in which the miR-21 surge was antagonized by miR-21-ASO, the number of hepatocytes in S phase at 36 hours after 2/3 PH was markedly reduced as compared to controls. In addition, our finding that the hepatocyte cell cycle defect in miR-21-ASO-injected mice phenocopied that of mice in which cyclin D1 was suppressed with *Ccnd1*-ASO further suggests that miR-21's effect on hepatocyte cell cycle progression in early liver regeneration is mainly mediated by cyclin D1. However, hepatocyte cell cycle progression was not permanently blocked in miR-21-ASO-injected mice and the cells eventually entered S phase and restored the lost liver mass. Impaired hepatocyte proliferation, particularly if it is caused by single gene deficiencies, is typically compensated for in liver regeneration. Compensation is the result of redundant signaling pathways providing the missing function, which leads to delayed rather than failed liver mass restoration (20). A previous study suggested that overexpression of cyclin E can compensate for lack of cyclin D1 in *Ccnd1*^{-/-} mice, thereby facilitating normal hepatocyte proliferation (65). In accordance with this result, we found that cyclin E1 and downstream cyclins involved in liver regeneration were

overexpressed as early as 18 hours after 2/3 PH, when cyclin D1 protein deficiency was most prominent in miR-21-depleted hepatocytes. In addition, we observed that cyclin D1 translation was slowly improving between 18 and 36 hours after 2/3 PH. Because miR-21 was still depleted at 36 hours after 2/3 PH, the finding suggests miR-21-independent cyclin D1 translation as another mechanism that helps rescue liver regeneration in miR-21-ASO-injected mice.

2.4 Figures and Tables

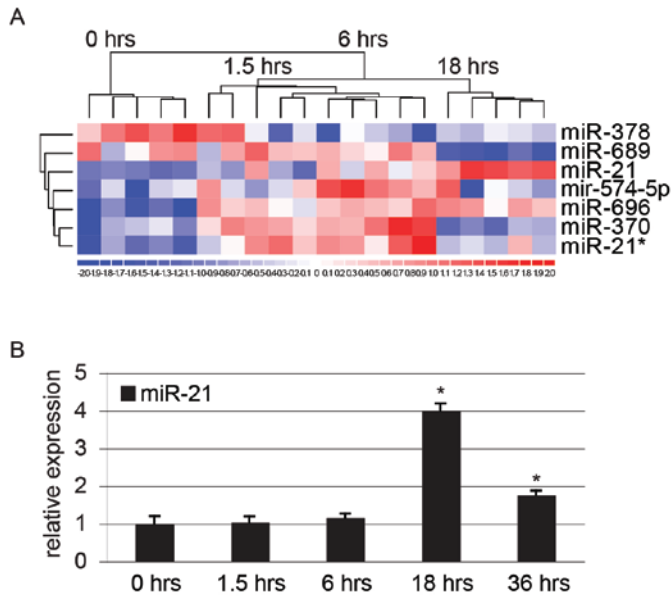


Figure 1 miRNA expression changes in livers of wildtype mice in response to 2/3 PH. **(A)** Heatmap of the miRNAs that are significantly differentially expressed in livers of wildtype mice during the first 18 hours after 2/3 PH. The miRNA clustering tree is shown on the left and the sample clustering tree appears at the top. The color scale in the bottom illustrates the relative expression level of a miRNA across all samples. Red color represents an expression level above mean, blue color represents expression lower than mean. The clustering is performed on \log_2 (Hy3/Hy5) ratios that passed the filtering criteria of $P < 0.001$ (Supplementary Table 1). **(B)** qRT-PCR shows that expression of miR-21 peaks at 18 hours after 2/3 PH in wildtype mice. Error bars represent \pm SEM. * $P < 0.005$.

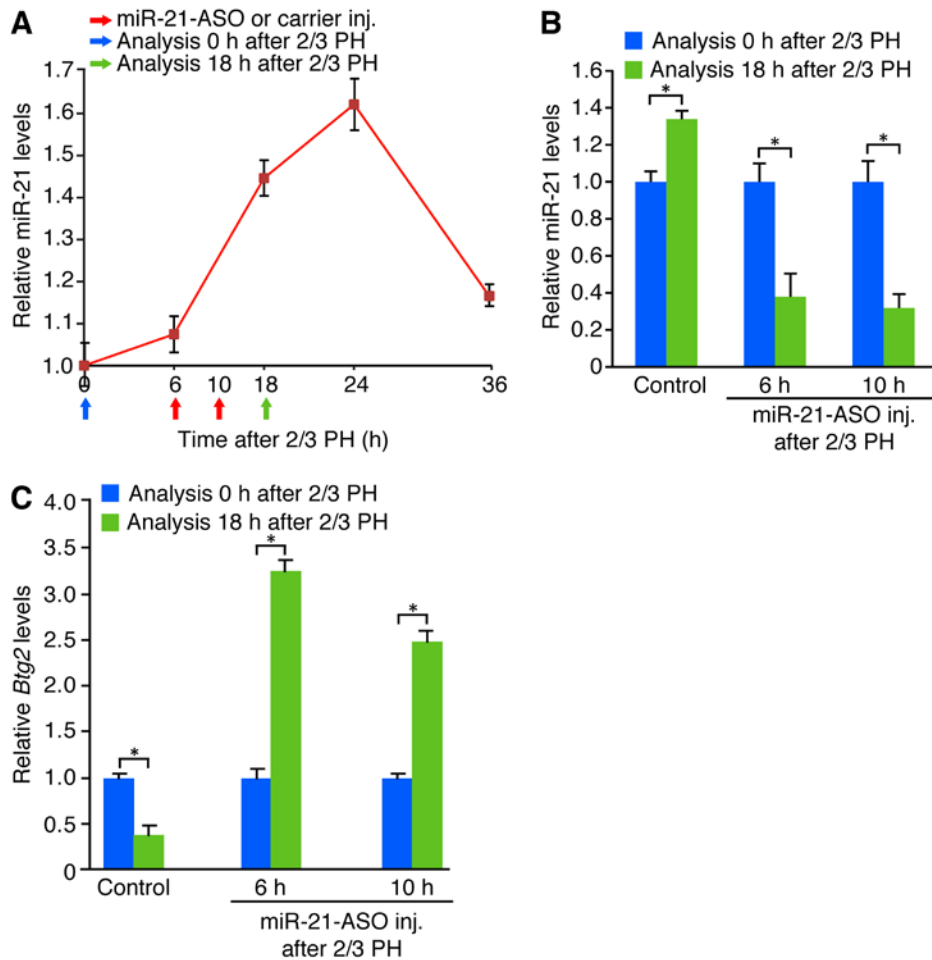


Figure 2 miR-21-ASO injected into the tail vein facilitates inhibition of increased miR-21 expression and de-repression of its target genes after 2/3 PH. **(A)** Time course of miR-21 expression after 2/3 PH. miR-21 levels were determined by quantitative reverse transcription-PCR (qRT-PCR). Arrows indicate time points of miR-21-ASO or carrier (Control) injection and liver analysis relative to 2/3 PH. Liver samples obtained by 2/3 PH (Analysis 0h after 2/3 PH) were used to define baseline levels in the quiescent liver. **(B)** qRT-PCR shows that miR-21-ASO injections at 6 or 10 hours after 2/3 PH are similarly effective in antagonizing the peak of the surge in miR-21 expression after 2/3 PH. **(C)** The repression of *Btg2* mRNA levels in livers of control mice after 2/3 PH is reversed in mice injected with miR-21-ASO at 6 or 10 hours after 2/3 PH. At least 3 mice were analyzed for each time point and treatment. Control mice were injected with carrier. Data represent mean \pm SEM. * $P < 0.05$.

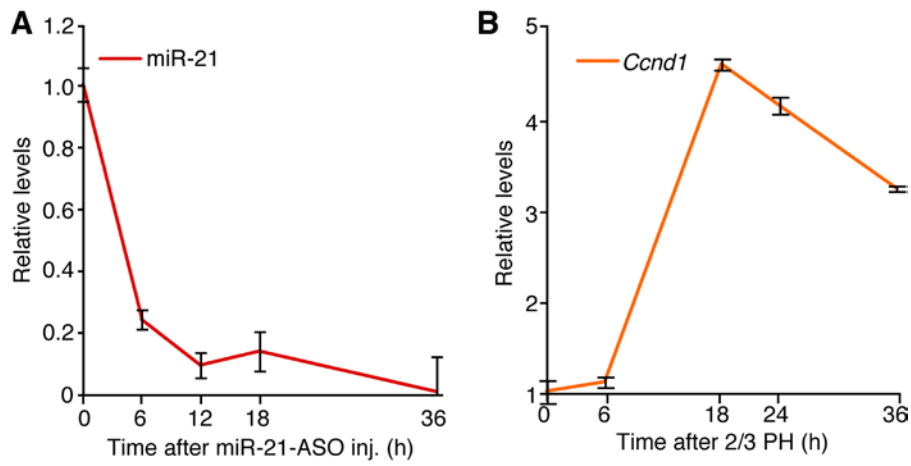


Figure 3 Time course of miR-21 and *Ccnd1* levels in livers of mice after miR-21-ASO injection or 2/3 PH. (A) Time course of miR-21 levels after a single tail vein injection of miR-21-ASO.(B) Time course of *Ccnd1* mRNA levels after 2/3 PH. At least 3 mice were analyzed for each time point and treatment. Data represent mean \pm SEM.

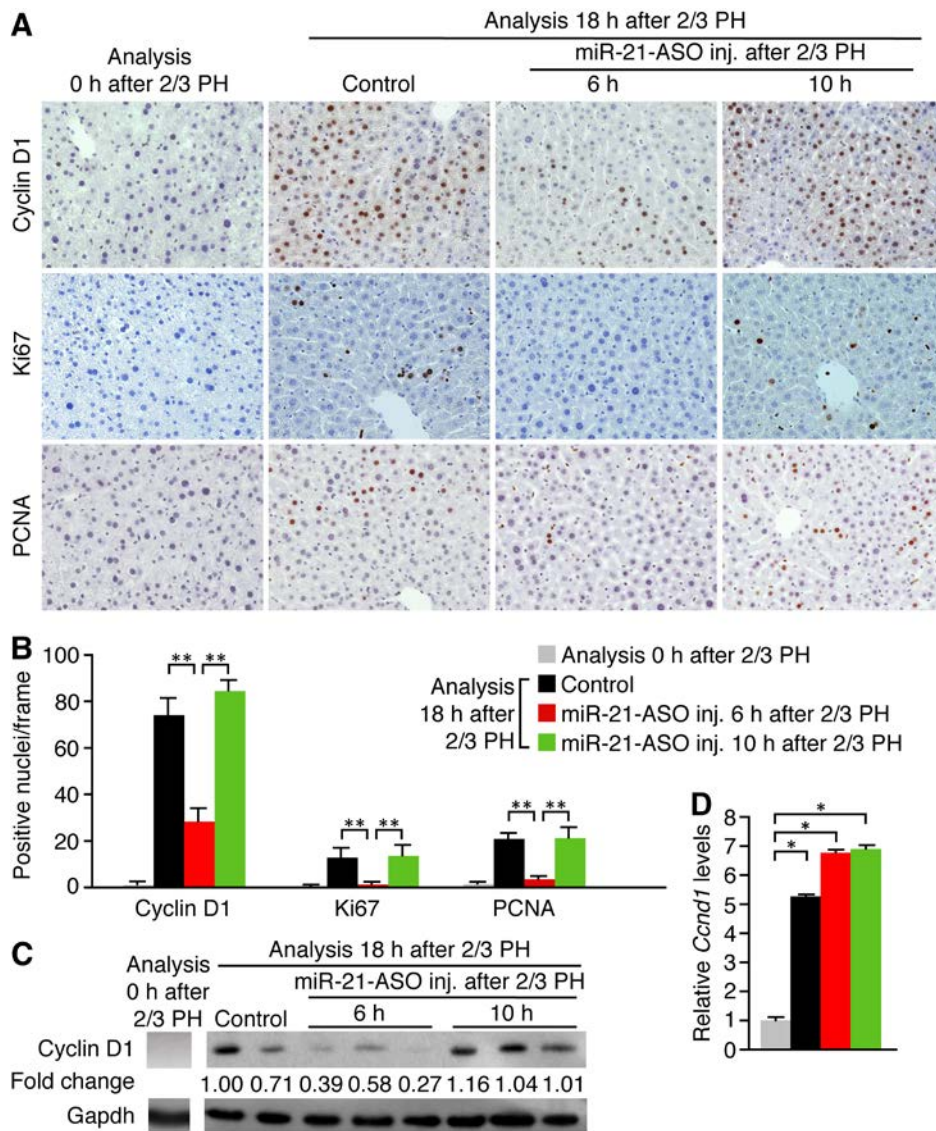


Figure 4 Inhibition of miR-21 decreases cyclin D1 protein but not mRNA in hepatocytes after 2/3 PH. (A) Immunostainings show that hepatocytes are normally quiescent but proliferate at 18 hours after 2/3 PH in control mice. Hepatocytes of mice injected with miR-21-ASO at 6 hours, but not at 10 hours, after 2/3 PH fail to express markers of progression through G1 (cyclin D1 and Ki67, brown) and into S (Ki67 and PCNA, brown) phase of the cell cycle. (B) Quantification of hepatocytes expressing markers of cell cycle progression. For each immunostaining, approximately 1,500 hepatocytes (250 per frame) were analyzed per time point and treatment. (C) Immunoblotting shows failure to increase cyclin D1 protein levels in livers of mice injected with miR-21-ASO at 6 hours, but not at 10 hours, after 2/3 PH. Numbers indicate protein levels relative to controls. Gapdh was analyzed as a loading control. (D) qRT-PCR shows that miR-21-ASO injection does not interfere with induction of liver *Ccnd1* transcription after 2/3 PH. At least 3 mice were analyzed for each time point and treatment. No differences were observed between control mice injected with carrier at 6 versus 10 hours after 2/3 PH. Data represent mean \pm SEM. * P < 0.05, ** P < 0.01.

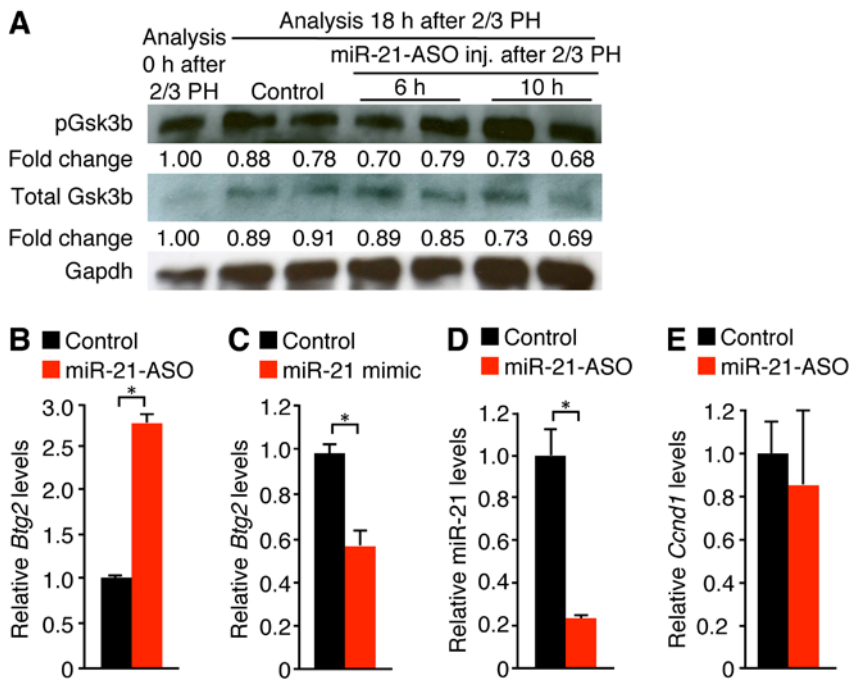


Figure 5 miR-21 promotes expression of cyclin D1 by facilitating its translation, not by preventing its degradation. **(A)** Phosphorylation at Ser9 prevents Gsk3b from triggering proteosomal degradation of cyclin D1. Immunoblotting shows that, 18 hours after 2/3 PH, the levels of Gsk3b phosphorylated at Ser9 (pGsk3b) are not increased in livers of mice injected with miR-21-ASO at 6 or 10 hours after 2/3 PH as compared to controls. Total Gsk3b protein levels are indistinguishable between controls and mice injected with miR-21-ASO at 6 hours after 2/3 PH and slightly decreased in mice injected with miR-21-ASO at 10 hours after 2/3 PH. Numbers indicate protein levels relative to time point 0 hours after 2/3 PH. At least 3 mice were analyzed for each time point and treatment. Control mice were injected with carrier. Gapdh was analyzed as a loading control. **(B and C)** qRT-PCR shows that transfection of miR-21-ASO or miR-21 mimic into Hepa1,6 cells increases or decreases *Btg2* mRNA levels, respectively. **(D)** qRT-PCR shows 5-fold suppression of miR-21 48 hours after transfection with miR-21-ASO in Hepa1,6 cells used for polysome analysis. **(E)** qRT-PCR shows *Ccnd1* mRNA levels are unaltered in Hepa1,6 cells 48 hours after transfection with miR-21-ASO. Data represent mean \pm SEM. * $P < 0.05$.

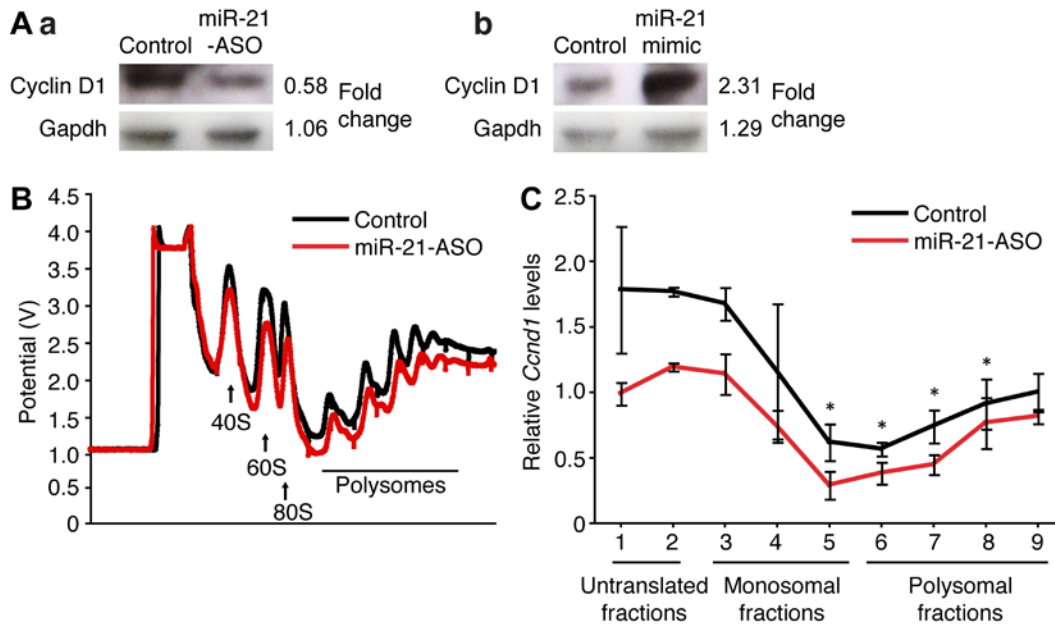


Figure 6 miR-21 regulates cyclin D1 translation. (A) Transfection of 40 nM miR-21-ASO decreases cyclin D1 levels in Hepa1,6 cells approximately 2-fold (a). Transfection of 40 nM miR-21 mimic increases cyclin D1 levels in Hepa1,6 cells approximately 2-fold (b). Results representative of 3 separate experiments are shown. (B) Elution profile of fractionated cytoplasmic lysates from Hepa1,6 cells transfected with miR-21-ASO or non-targeting ASO (Control). Untranslated fractions, containing 40S or 60S ribosomal subunits, are eluted first, followed by monosomal fractions containing 80S single intact ribosomes and polysomal fractions containing multiple associated ribosomes. Absorbance readings at 254 nm were automatically converted into potential values, which were plotted against the eluted fractions. (C) qRT-PCR shows that *Ccnd1* mRNA levels in RNA isolated from the actively translated polysomal fractions are lower in miR-21-ASO-transfected cells than in control cells. Relative levels of *Ccnd1* mRNA in fractions were determined by normalization to *Gapdh*. These values were further normalized to *Ccnd1* mRNA levels in unfractionated samples to account for potential differences in starting cell numbers. Data represent mean \pm SEM. * $P < 0.05$.

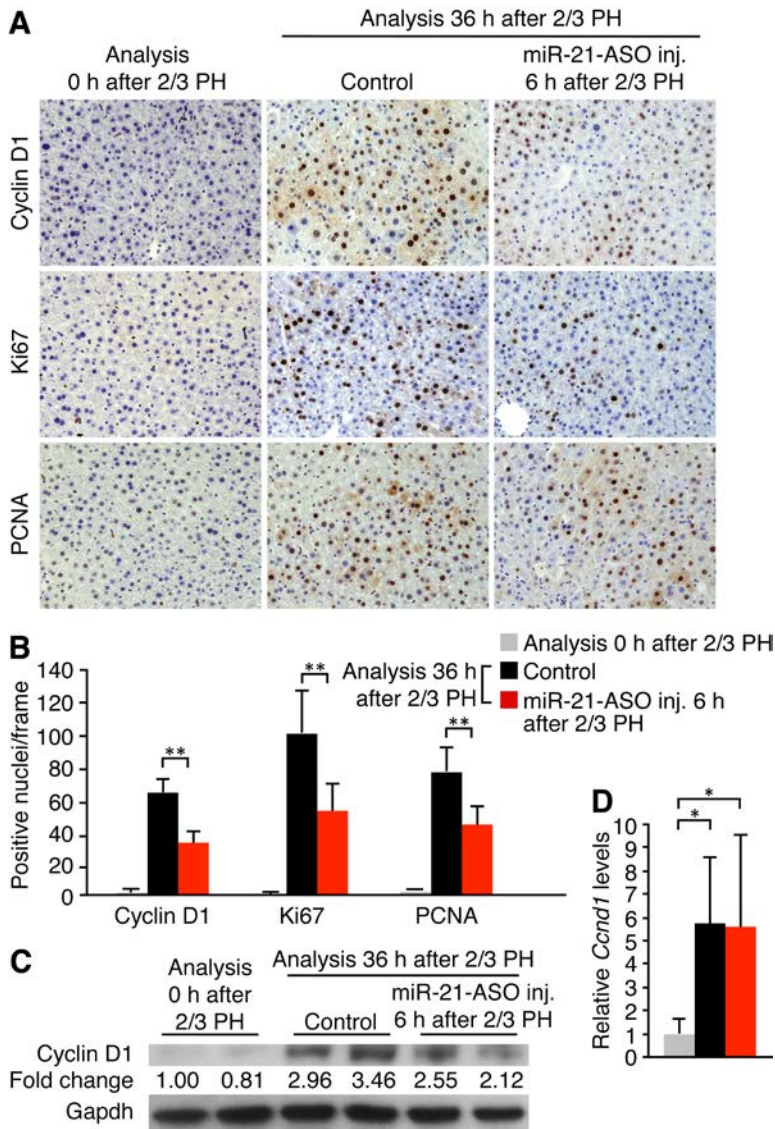


Figure 7 Inhibition of miR-21 delays S phase entry of hepatocytes after 2/3 PH. (**A** and **B**)

Quantification of Ki67 and PCNA immunostainings (both brown) shows that many hepatocytes have entered S phase at 36 hours after 2/3 PH in control mice. Significantly fewer hepatocytes stain positive for these markers or cyclin D1 (all brown) in mice injected with miR-21-ASO. For each immunostaining, approximately 1,500 hepatocytes (250 per frame) were analyzed per time point and treatment. (**C**) Immunoblotting shows lower cyclin D1 protein levels at 36 hours after 2/3 PH in livers of mice injected with miR-21-ASO as compared to controls. Numbers indicate protein levels relative to time point 0 hours after 2/3 PH. Gapdh was analyzed as a loading control. (**D**) qRT-PCR shows that miR-21-ASO injection does not interfere with induction of liver *Ccnd1* transcription at 36 hours after 2/3 PH. At least 3 mice were analyzed for each time point and treatment. miR-21-ASO was injected at 6 hours after 2/3 PH. Control mice were injected with carrier at 6 hours after 2/3 PH. Data represent mean \pm SEM. * $P < 0.05$, ** $P < 0.01$.

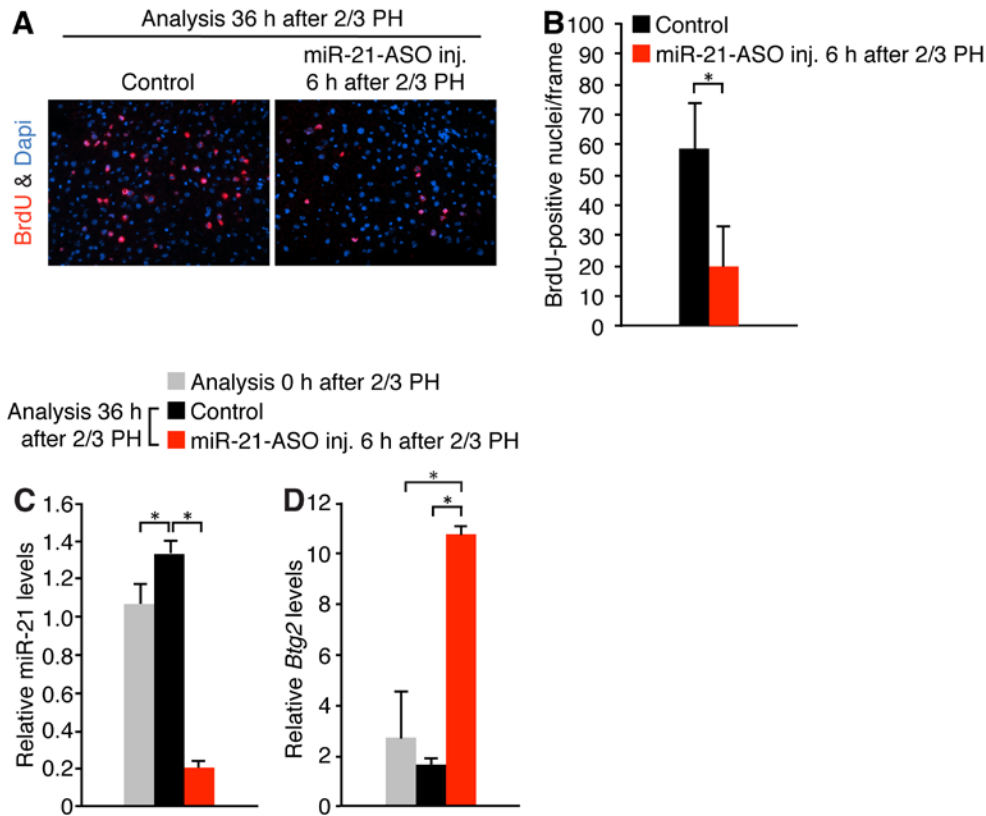


Figure 8 Impaired S phase entry and miR-21 depletion 36 hours after 2/3 PH in hepatocytes of miR-21-ASO-injected mice. (A and B) BrdU immunostaining shows that many hepatocytes synthesize DNA 36 hours after 2/3 PH in control mice. Significantly fewer hepatocytes are BrdU-positive in mice injected with miR-21-ASO. Approximately 1,500 hepatocytes (250 per frame) were analyzed for each treatment. Original magnification, x200. (C) qRT-PCR shows strong inhibition of miR-21 36 hours after 2/3 PH in livers of miR-21-ASO-injected mice. (D) The repression of *Btg2* mRNA levels in livers of control mice 36 hours after 2/3 PH is reversed in mice injected with miR-21-ASO. At least 3 mice were analyzed for each time point and treatment. Control mice were injected with carrier at 6 hours after 2/3 PH. Data represent mean \pm SEM. * $P < 0.05$.

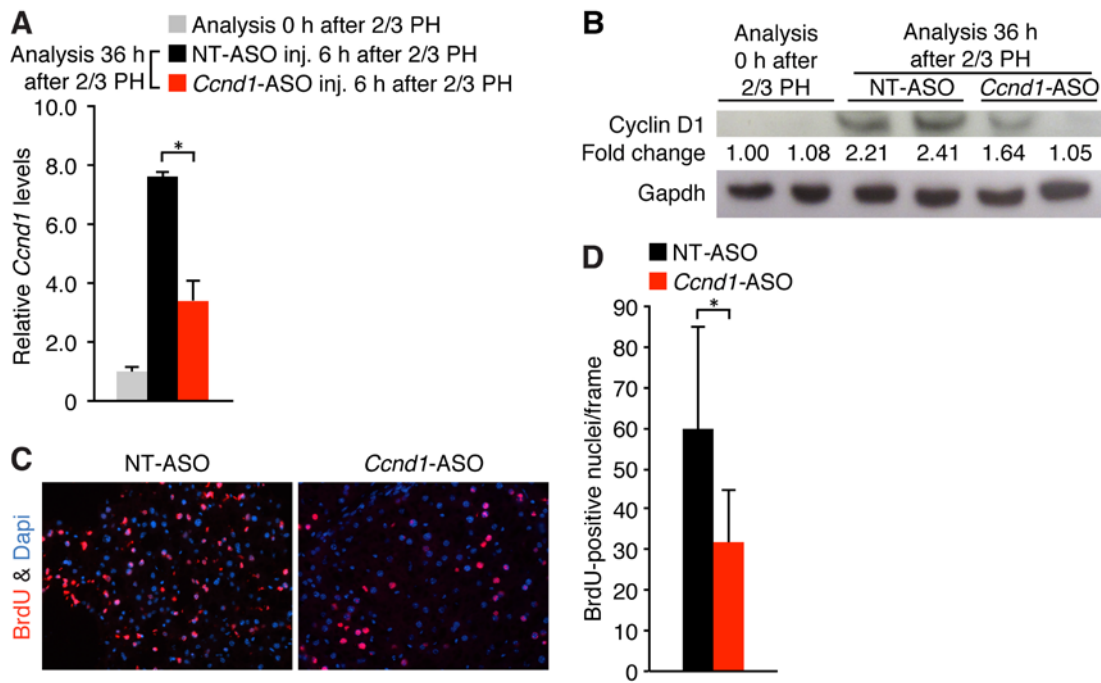


Figure 9 Knockdown of cyclin D1 in hepatocytes during the early phase of liver regeneration impairs S phase entry. (A-D) Comparison of liver cyclin D1 mRNA and protein levels and number of BrdU-positive hepatocytes at 36 hours after 2/3 PH between mice injected with *Ccnd1*-ASO and mice injected with control NT-ASO at 6 hours after 2/3 PH. qRT-PCR shows that *Ccnd1* mRNA levels are 2-fold lower in *Ccnd1*-ASO-injected mice than in NT-ASO-injected mice (A). Immunoblotting shows that cyclin D1 protein levels are also lower in *Ccnd1*-ASO-injected mice than in NT-ASO-injected mice. Numbers indicate protein levels relative to time point 0 hours after 2/3 PH. Gapdh was analyzed as a loading control (B). BrdU immunostaining shows that fewer hepatocytes are synthesizing DNA in *Ccnd1*-ASO-injected mice than in NT-ASO-injected mice (C). For quantification, approximately 1,500 hepatocytes (250 per frame) were analyzed for each treatment (D). At least 3 mice were analyzed for each time point and treatment. Original magnification, x200. Data represent mean \pm SEM. * $P < 0.05$.

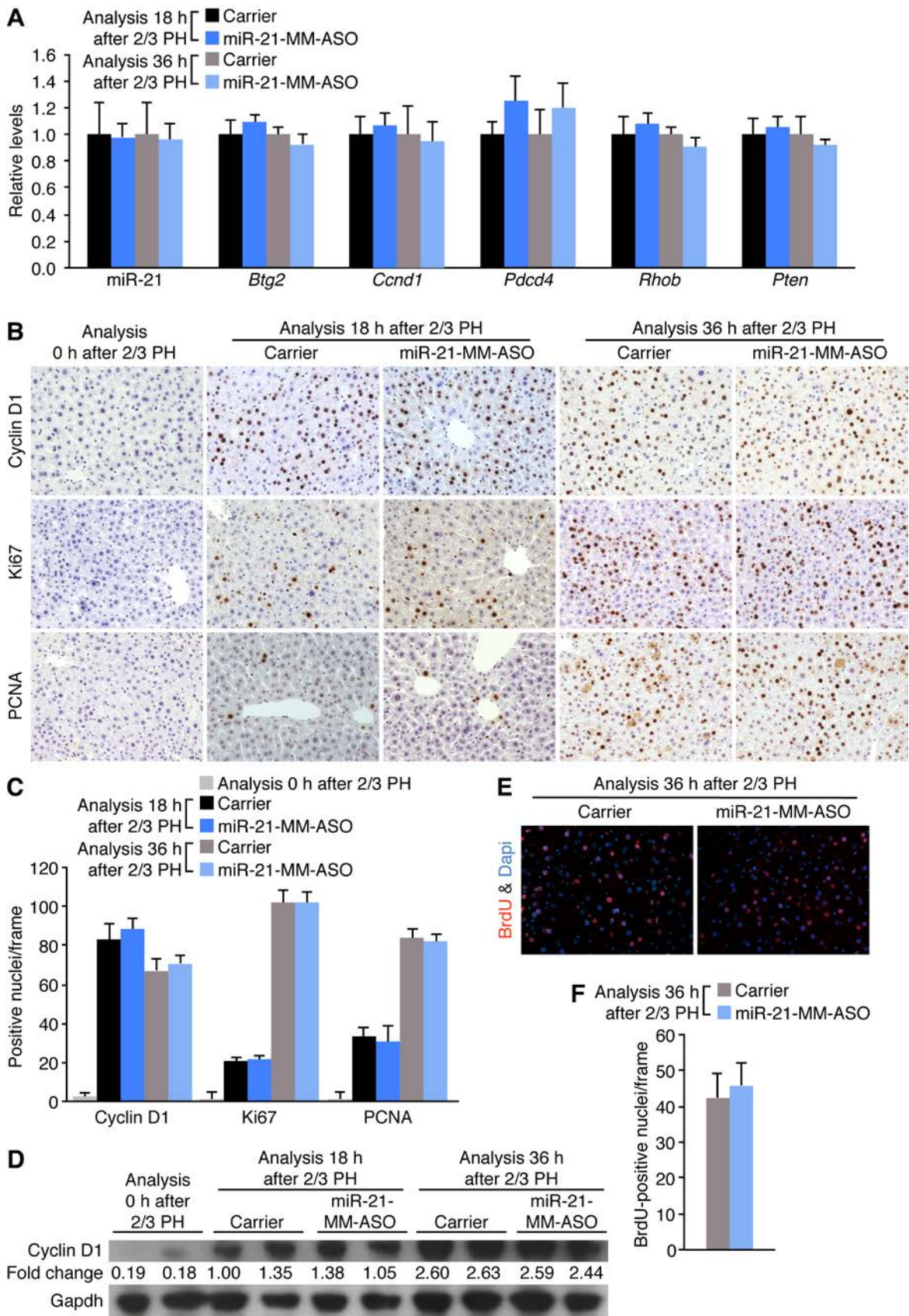


Figure 10 Impaired cyclin D1 translation and cell cycle progression of hepatocytes of miR-21-ASO-injected mice after 2/3 PH are not due to unspecific effects or toxicity caused by the ASO. (A-D) Mice

received tail vein injection of carrier or miR-21-MM-ASO at 6 hours after 2/3 PH; livers were analyzed at 18 or 36 hours after 2/3 PH. qRT-PCR shows that carrier and miR-21-MM-ASO injection have indistinguishable effects on expression of miR-21 and its target genes. Average carrier levels were set to 1 (**A**). Immunostainings show that the number of hepatocytes expressing markers of progression through G1 (cyclin D1 and Ki67, brown) and into S (Ki67 and PCNA, brown) phase of the cell cycle is indistinguishable between mice injected with carrier and mice injected with miR-21-MM-ASO (**B**). Quantification of hepatocytes expressing markers of cell cycle progression (**C**). Immunoblotting shows that cyclin D1 protein levels increase equally in mice injected with carrier and mice injected with miR-21-MM-ASO. Numbers indicate protein levels relative to carrier at time point 18 hours after 2/3 PH. Gapdh was analyzed as a loading control (**D**). (**E** and **F**) BrdU immunostaining shows a similar number of hepatocytes synthesizing DNA 36 hours after 2/3 PH in mice injected with carrier and mice injected with miR-21-MM-ASO at 6 hours after 2/3 PH. For each immunostaining, approximately 1,500 hepatocytes (250 per frame) were analyzed per time point and treatment. At least 3 mice were analyzed for each time point and treatment. Original magnification, x200. Data represent mean \pm SEM.

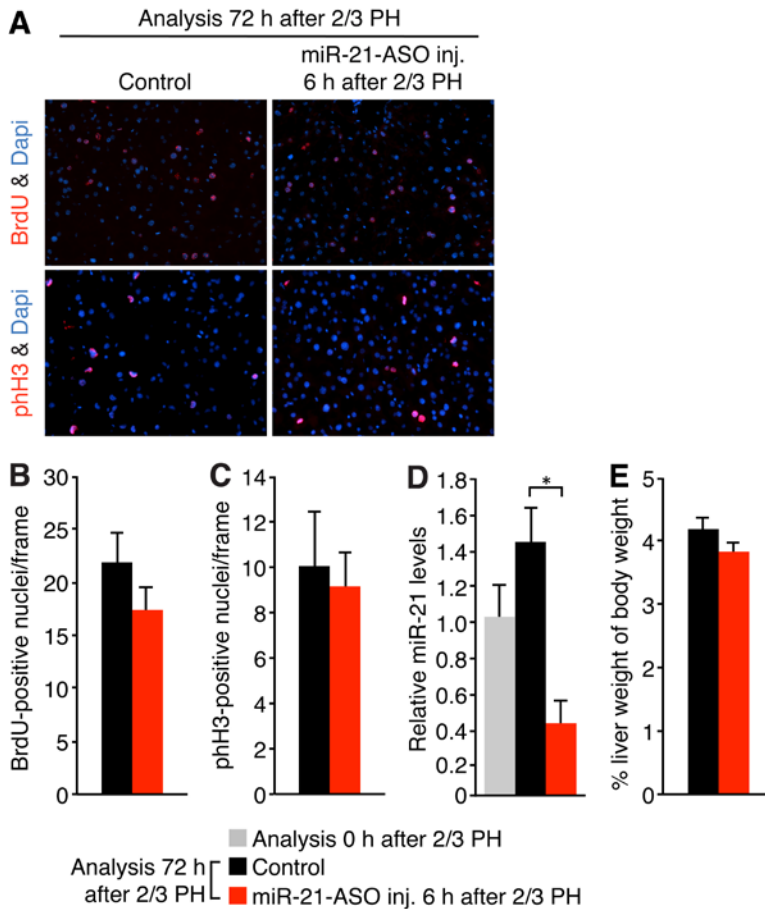


Figure 11 Normal mitosis and liver mass restoration despite miR-21 depletion 72 hours after 2/3 PH in hepatocytes of miR-21-ASO-injected mice. (A-C) BrdU and pH3 immunostainings. BrdU immunostaining shows a similar number of hepatocytes synthesizing DNA in miR-21-ASO-injected and control mice 72 hours after 2/3 PH (A and B). pH3 immunostaining shows a similar number of hepatocytes in mitosis in miR-21-ASO-injected and control mice 72 hours after 2/3 PH (A and C). For each immunostaining, approximately 1,500 hepatocytes (250 per frame) were analyzed per treatment. Original magnification, x200. (D) qRT-PCR shows that miR-21 is still inhibited in livers of miR-21-ASO-injected mice 72 hours after 2/3 PH. (E) The extent of liver mass restoration 72 hours after 2/3 PH is similar in mice injected with miR-21-ASO and control mice. At least 3 mice were analyzed for each time point and treatment. Control mice were injected with carrier at 6 hours after 2/3 PH. Data represent mean \pm SEM. * $P < 0.05$.

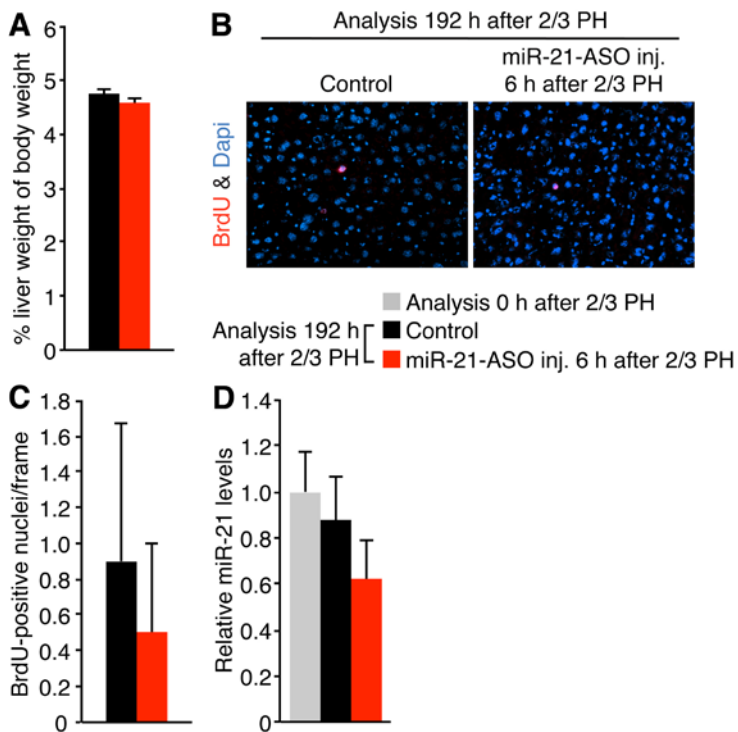


Figure 12 Complete liver mass restoration 192 hours after 2/3 PH in miR-21-ASO-injected mice. **(A)** The liver to body weight ratio is indistinguishable between miR-21-ASO-injected mice and control mice 192 hours after 2/3 PH. **(B and C)** BrdU immunostaining shows a similarly small number of hepatocytes synthesizing DNA in miR-21-ASO-injected mice and control mice 192 hours after 2/3 PH. Approximately 1,500 hepatocytes (250 per frame) were analyzed for each treatment. Original magnification, x200. **(D)** qRT-PCR shows near-complete normalization of miR-21 levels in miR-21-ASO-injected mice 192 hours after 2/3 PH. At least 3 mice were analyzed for each time point and treatment. Control mice were injected with carrier at 6 hours after 2/3 PH. Data represent mean \pm SEM.

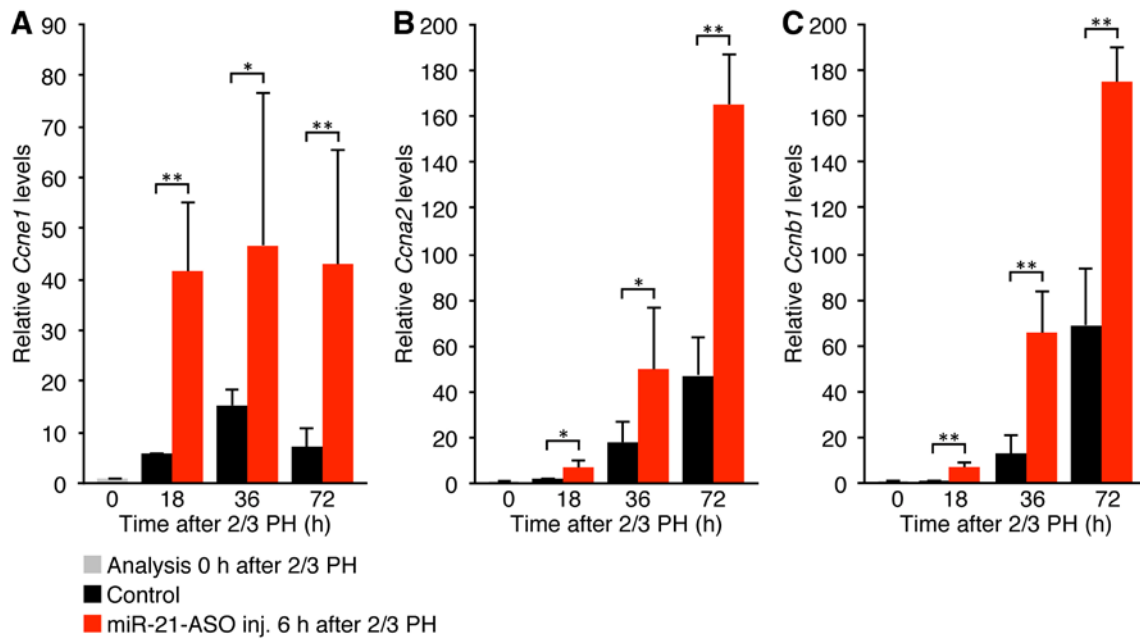


Figure 13 Overexpression of *Ccne1*, *Ccna2* and *Ccnb1* in miR-21-ASO-injected mice. (A-C) qRT-PCR shows that *Ccne1* (A), *Ccna2* (B) and *Ccnb1* (C) mRNA levels are induced from 18 to 72 hours after 2/3 PH in miR-21-ASO-injected mice as compared to control mice. At least 3 mice were analyzed for each time point and treatment. Control mice were injected with carrier at 6 hours after 2/3 PH. Data represent mean \pm SEM. * $P < 0.05$, ** $P < 0.01$.

Chapter 3: miR-21 suppresses Rhob in the regenerating liver

3.1 Introduction

In the previous chapter, we established that miR-21 inhibition during early liver regeneration can reduce cyclin D1 translation leading to delayed hepatocyte cell cycle entry into S phase. miRNAs are short RNAs that post-transcriptionally regulate the expression of target genes by binding to the target mRNAs. Although a large number of animal miRNAs has been defined, only a few targets are known. Animal miRNAs, in contrast to plant miRNAs which usually bind nearly perfectly to their targets, bind less tightly, with a few nucleotides being unbound, thus producing more complex secondary structures of miRNA/target duplexes. The combinatorial nature of secondary structure formation, that is, the huge number of possible bindings as a result of loops of unpaired nucleotides, makes prediction of miRNA targets by simple pattern matching or BLAST searches impossible(68). However, in recent years, a variety of miRNA target prediction algorithms such as PicTar, Targetscan, DIANA-microT, miRanda and rna22 have become available(69-71). Unfortunately, the results from these algorithms are often inconsistent(70). Hence, it is still a difficult task to find a functional miRNA target and direct validation of miRNA target genes is required. Experimental validation of putative target genes are often based on (1) quantification of a luciferase reporter construct linked to the 3' UTR of the putative target gene after introduction of a miRNA into the cell, or (2) monitoring mRNA levels of the putative target gene in the cell after overexpression or inhibition of a miRNA(72). After confirming the miRNA:mRNA interaction, site-directed mutagenesis of the 3' UTR within the reporter construct can be integrated into the reporter assay to validate the results and identify the miRNA recognition elements. In our case, the problem of correctly identifying miR-21 putative target genes was partially overcome by putting the list of predicted target genes through a gene ontology analysis to further sift out genes which do not function as negative regulators of cell cycle. Using this strategy, we managed to narrow down a list of 63 predicted miR-21 target genes to 6 genes which function as negative regulators of cell cycle and/or cellular functions. This allowed us to functionally test these 6 genes to

identify *Rhob*, a tumor suppressor gene that plays an important role in cell proliferation and migration, as a true target of miR-21.

3.2 Results

After confirming that miR-21 promotes hepatocyte proliferation during liver regeneration, we sought to identify the mechanism of how miR-21 facilitates cyclin D1 translation in the early phase of liver regeneration. Few instances have been reported where a miRNA directly enhances the translation of a target gene (73, 74). Because we failed to detect the necessary miR-21 binding sites in the message of *Ccnd1* (data not shown), we reasoned that miR-21 promotes cyclin D1 translation indirectly by targeting a cell cycle inhibitor. Thus, we used gene ontology analysis (75) to identify candidate genes that negatively regulate the cell cycle among 63 genes previously predicted to be highly probable targets of miR-21 (Table 1) (55).

One of the candidate genes, programmed cell death protein 4 (*Pdcd4*), is an established target of miR-21 in cancer cells (54). We found that miR-21 targets *Pdcd4* also in normal liver, as was evident from increased *Pdcd4* mRNA levels in livers of mice at 6 hours after tail vein injection of miR-21-ASO (Figure 15A). Moreover, we found that the surge in miR-21 expression induced by 2/3 PH was associated with a decrease in *Pdcd4* mRNA levels (Figure 14B). However, *Pdcd4* protein levels were increased at 6 hours after 2/3 PH and only moderately decreased at 18 hours after 2/3 PH (Figure 14C), which suggests that *Pdcd4* is not effectively suppressed by miR-21 in the regenerating liver. Because of this result and, more importantly, previous findings that *Pdcd4* overexpression does not affect cyclin D1 mRNA or protein levels (76), we reasoned that *Pdcd4* de-repression is not the cause of impaired cyclin D1 translation in hepatocytes of miR-21-ASO-injected mice. Therefore, we focused our investigations on *Rhob*, the candidate gene with the highest probability of targeting by miR-21 (Table 1). *Rhob* is a GTPase that functions as a tumor suppressor by inhibiting cancer cell proliferation, migration and survival (77). We found that both *Rhob* mRNA and protein levels were inversely

correlated with the expression of miR-21 after 2/3 PH (Figure 15A). Bioinformatic analysis revealed that the 3' UTR of *Rhob* contains a highly probable miR-21 binding site that is conserved in mammalian species (Figure 15B). In support of this prediction, we found that tail vein injection of miR-21-ASO into mice caused increased *Rhob* mRNA levels in the liver 6 hours later (Figure 15C). To prove that the inverse correlation between miR-21 and *Rhob* expression *in vivo* was due to direct interaction, we investigated whether miR-21 targets *Rhob* in Hepa1,6 cells *in vitro* (Figure 15D). Indeed, we found that *Rhob* mRNA levels and the activity of a luciferase reporter gene linked to the 3' UTR of mouse *Rhob* decreased or increased in response to transfection of miR-21 mimic or inhibitor, respectively. Mutation of the miR-21 binding site in *Rhob*'s 3'UTR completely abolished the ability of miR-21 mimic and inhibitor to regulate luciferase activity, further confirming *Rhob* as a direct target of miR-21 (Figure 15D). The conservation of *Rhob* targeting by miR-21 is further supported by a recent study showing that miR-21 promotes the defining features of the metastatic phenotype, migration, elongation and invasion, by inhibiting the human gene in a breast cancer cell line (50). Viewed together, our findings suggest that *Rhob* is directly suppressed by the surge in miR-21 expression occurring in the early phase of liver regeneration.

3.3 Discussion

In this chapter, we identified *Rhob* as a target gene of miR-21. Using a combination of bioinformatics prediction and gene ontology analysis, we narrowed down 63 predicted target genes to 6 genes. We then chose to focus on *Rhob* because, of the 6 predicted miR-21 target genes with established proliferation-inhibiting function, *Rhob* had one of the highest scores and free energy, and was shown to be a conserved miR-21 target gene in both mice and humans by multiple sequence alignment. *Rhob* has also been shown to function as a tumor suppressor gene that plays an important role in cell proliferation and migration by regulating diverse cellular processes, including cytoskeletal organization, gene transcription and cytokinesis (78-80). Our data shows that *Rhob* mRNA and protein levels correlate inversely with miR-21 levels after 2/3 PH. In addition, *in vitro* studies performed using a

mouse hepatoma cell line show that transfection of miR-21 mimic can lower endogenous Rhob mRNA levels. Transfection of miR-21 mimic can also reduce luciferase protein expression when the 3' UTR of Rhob was cloned downstream of the luciferase gene. Conversely, addition of miR-21-ASO led to an increase in endogenous Rhob levels and also rescued the decrease in luciferase activity caused by miR-21 mimic. These results confirm that Rhob is a target gene of miR-21. Since Rhob has not been shown to directly regulate translation, an analysis of Rhob and its downstream signaling targets was required to elucidate the link between Rhob and cyclin D1 translation.

3.4 Figures and Tables

Accession	Symbol	Gene name
NM_007483	<i>Rhob</i>	Ras homolog gene family, member B
NM_011446	<i>Sox7</i>	SRY-box containing gene 7
NM_016678	<i>Reck</i>	Reversion-inducing cysteine-rich protein with Kazal motifs
NM_001168491	<i>Pdcd4</i>	Programmed cell death protein 4
NM_177687	<i>Crebl2</i>	cAMP-responsive element-binding protein-like 2
NM_009741	<i>Bcl2</i>	B-cell leukemia/lymphoma 2

Table 1 Predicted miR-21 target genes that are negative regulators of the cell cycle. 63 target genes of miR-21 predicted by both the TargetScan and the PicTar algorithm (55) were functionally categorized using g:Profiler gene ontology analysis (75). The 6 genes in the category “negative regulators of the cell cycle” are shown. Genes are listed in order of decreasing probability of targeting by miR-21.

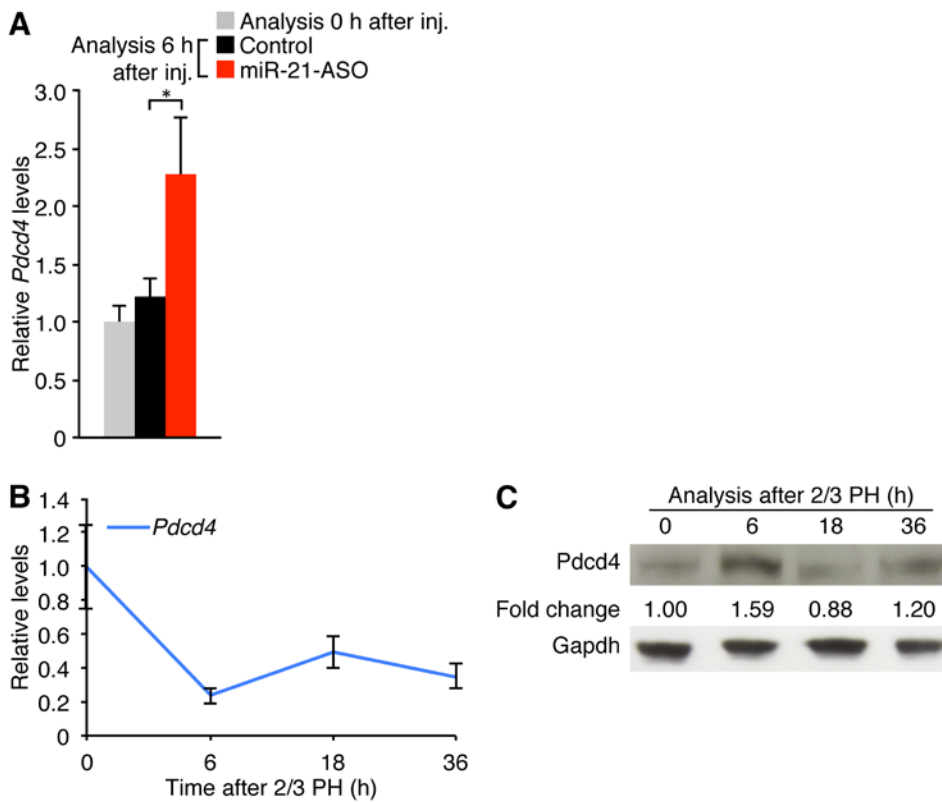


Figure 14 Moderate suppression of the miR-21 target *Pdc4* in early liver regeneration. **(A)** qRT-PCR shows a 2-fold increase in *Pdc4* mRNA levels in livers of mice 6 hours after a single tail vein injection of miR-21-ASO. Control mice were injected with carrier. **(B)** qRT-PCR shows a rapid and continuous decrease in *Pdc4* mRNA levels after 2/3 PH. **(C)** Immunoblotting shows that *Pdc4* protein levels undulate after 2/3 PH and are moderately decreased at 18 hours after 2/3 PH when miR-21 expression peaks. Numbers indicate protein levels relative to time point 0 hours after 2/3 PH. *Gapdh* was analyzed as a loading control. At least 3 mice were analyzed for each time point and treatment. Data represent mean \pm SEM. * $P < 0.05$.

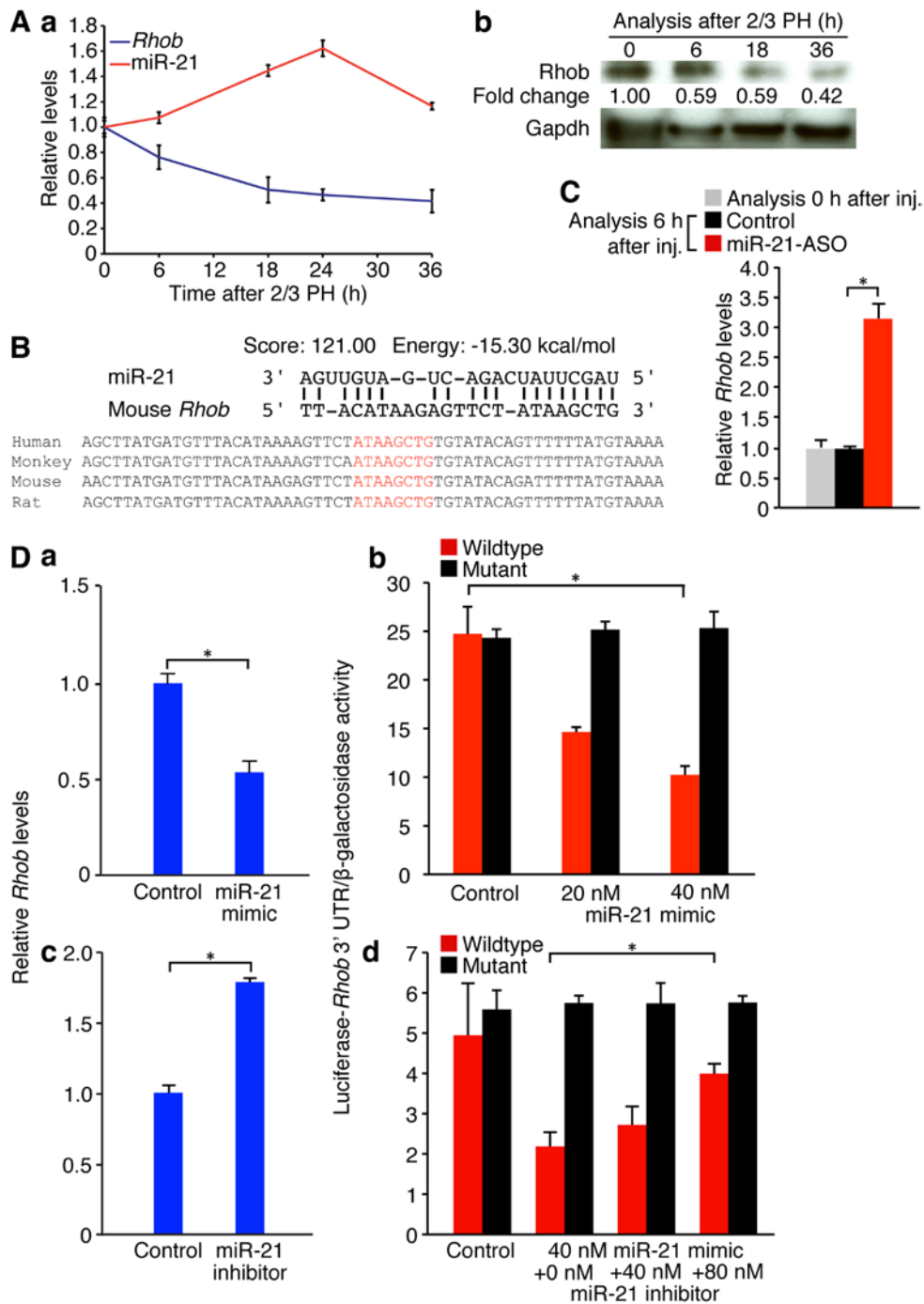


Figure 15 Induction of miR-21 in liver regeneration decreases Rhob expression by direct targeting. (A) Inverse correlation of miR-21 and Rhob expression levels after 2/3 PH. Induction of miR-21 after 2/3 PH is associated with decreased *Rhob* mRNA (a) and protein (b) levels. Numbers indicate protein levels relative to time point 0 hours after 2/3 PH. Gapdh was analyzed as a loading control. (B) High prediction score and favorable binding energy suggest that miR-21 targets the 3' UTR of *Rhob*. The complementary sequence in the *Rhob* 3' UTR and the seed region of miR-21 (red letters) is conserved between mammalian species. (C) *Rhob* mRNA levels in the liver are increased 6 hours after a single tail vein injection of miR-21-ASO. Control mice were injected with carrier. At least 3 mice were

analyzed for each time point and treatment. **(D)** Direct inhibition of Rhob by miR-21. Transfection of miR-21 mimic into Hepa1,6 cells decreases *Rhob* mRNA levels **(a)**. The activity of a luciferase reporter gene linked to the *Rhob* 3' UTR is inhibited by miR-21 mimic in a dose-dependent fashion. This effect was completely abolished by mutating the miR-21 binding site in *Rhob* 3' UTR **(b)**. Conversely, transfection of miR-21 inhibitor into Hepa1,6 cells increases *Rhob* mRNA levels **(c)**.

Chapter 4: miR-21 promotes cyclin D1 translation and cell cycle progression in early liver regeneration by suppressing Rhob and promoting Akt1-mediated activation of mTORC1

4.1 Introduction

In the previous chapters, we have shown that miR-21 inhibition leads to decreased cyclin D1 translation which leads to delayed hepatocyte cell cycle entry. We have also shown that Rhob is a target gene of miR-21. Rho proteins are Ras superfamily GTPases that regulate actin cytoskeleton, cell adhesion, motility, proliferation and apoptosis (81, 82). In higher vertebrates, there are three different Rho GTPases, RhoA, RhoB and RhoC, which share 85% amino acid sequence identity (83). However, Rhob is located in a different cellular compartment as RhoA and has a unique function in cells. Rhob is located in early-endosome and nuclear membranes and has a specialized function related to intracellular trafficking of cytokine receptors such as EGF receptor (EGFR) (84). Importantly, Rhob can also inhibit the cell cycle and its expression can be upregulated in response to cell stress (85, 86). In cultured cells, Rhob expression is induced by a variety of stimuli such as UV irradiation, cytokines or growth factors (87). Rhob levels also vary through the cell cycle and the protein has a short half life of approximately 30 minutes (88). Rhob has also been shown to regulate diverse cellular processes, including cytoskeletal organization, gene transcription and cytokinesis (78-80). Furthermore, Rhob has been shown to antagonize Ras/PI3K/Akt malignancy (89). Overexpression of Rhob inhibits Akt-dependent cell transformation, migration and invasion in an animal model (89). Since activation of Akt leads to the phosphorylation of mTOR which has been shown to affect cell growth and survival, we hypothesized that it might be possible that Rhob signals through the Akt/mTOR pathway (31). In addition, mTOR has emerged as a major effector of cell growth and proliferation via the regulation of protein synthesis, in particular protein translation, through a large number of downstream targets (32,

33). Hence, these previous studies led us to investigate whether Rhob can antagonize the Akt/mTOR pathway and thus inhibit cap-dependent translation of cyclin D1.

4.2 Results

Rhob inhibits cyclin D1 translation by preventing Akt1-mediated activation of mTORC1. After confirming Rhob as a direct target of miR-21, we investigated whether Rhob inhibition is responsible for miR-21's effect on cyclin D1 translation. Although Rhob had not been implicated in the regulation of cyclin D1 expression, several lines of evidence suggested this possibility: First, Rhob inhibits activating phosphorylation of Akt1 (90, 91). Then, activated Akt1 regulates cyclin D1 expression through mTORC1 (92, 93). Finally, mTORC1 promotes assembly of the eIF-4F complex, which mediates translation initiation of genes like *Ccnd1* (34, 92). In fact, mTORC1 has been shown to be needed for eIF-4F assembly and cyclin D1 translation in hepatocytes after 2/3 PH (17, 94). Further considering that Akt1 activation is critical for the early phase of liver regeneration (95), we hypothesized that miR-21 facilitates rapid cyclin D1 translation in liver regeneration by relieving Akt1, and thus mTORC1, from inhibition by Rhob. To test this hypothesis, we overexpressed Rhob by transient plasmid transfection in Hepa1,6 cells that normally express Rhob at low levels (Figure 16A and Figure 17A). We used immunoblotting to determine the effects on cyclin D1 and Akt1. Moreover, as a read-out for mTORC1-mediated activation of eIF-4F-dependent translation initiation, we measured phosphorylation of 4E-BP1. mTORC1 initiates 4E-BP1 phosphorylation, which disables its ability to bind and inhibit eIF-4E and thus facilitates eIF-4F complex assembly (34, 92).

We found that overexpression of Rhob decreased cyclin D1 protein levels and levels of Akt1 activated by phosphorylation (Figure 16A). Moreover, as evidence for impaired mTORC1 activity, we found decreased inhibitory phosphorylation of 4E-BP1. In accordance with the hypothesized mechanism, Rhob overexpression decreased cyclin D1 protein but not *Ccnd1* mRNA levels (Figure 17B). To

confirm these results, we transfected Hepa1,6 cells with both the plasmid overexpressing Rhob and a plasmid inhibiting Rhob by RNA interference (RNAi). This resulted in decreased *Rhob* mRNA and protein levels, which caused increased levels of cyclin D1 protein and activated Akt1 (Figure 16A and Figure 17C). As expected, phosphorylation of 4E-BP1 was increased in response to Akt1 activation. Moreover, *Ccnd1* mRNA levels were not altered and thus dissociated from cyclin D1 protein levels (Figure 17D). Rhob overexpression or knockdown similarly inhibited or activated another target of mTORC1, S6 kinase 1 (S6K1) (Figure 17, E and F). These results reveal that Rhob inhibits eIF-4F-mediated initiation of cyclin D1 translation by preventing activation of Akt1 and its downstream mediator mTORC1.

miR-21 promotes cyclin D1 translation in early liver regeneration by suppressing Rhob. To further confirm that miR-21's ability to promote cyclin D1 translation was mediated by Rhob, we knocked down both miR-21 and Rhob in Hepa1,6 cells and examined cyclin D1 protein levels. We found that the decreased cyclin D1 protein levels observed in cells transfected with miR-21-ASO alone normalized after additional Rhob RNAi (Figure 16B and Figure 17G), which establishes Rhob as the critical target of miR-21 in promotion of cyclin D1 translation. We also performed cell cycle analysis using the same cells and showed that introduction of miR-21-ASO causes accumulation of cells in G1 phase and a corresponding decrease of cells in S phase whereas Rhob knockdown can ameliorate this phenotype, further confirming Rhob's ability to repress cell cycle progression (Figure 16C).

Finally, we determined whether miR-21 prevents Rhob from inhibiting Akt1/mTORC1 signaling and thus cyclin D1 translation in early liver regeneration. Our initial analyses showed that miR-21-ASO injection at 6 hours after 2/3 PH impaired expression of cyclin D1 in the liver at 18 and 36 hours after 2/3 PH (Figure 4, A-C and Figure 7, A-C). When we analyzed these samples further, we found that 2/3 PH suppressed Rhob, activated Akt1 and inhibited 4E-BP1 in control mice and miR-21-MM-ASO injected mice, but not in mice injected with miR-21-ASO 6 hours after 2/3 PH (Figure 16, D and E and

Figure 17H). To ascertain that miR-21 regulates Akt1/mTORC1 signaling in liver regeneration through Rhob, we analyzed the expression of phosphatase and tensin homolog (PTEN) because inhibition of PTEN by miR-21 was previously shown to cause Akt1 activation in cancer cells (53, 96). We found that miR-21 targets PTEN in normal liver, as was evident from increased *Pten* mRNA levels at 6 hours after tail vein injection of miR-21-ASO into mice (Figure 18A). However, we also found that PTEN mRNA and protein levels markedly increased in the liver after 2/3 PH (Figure 18, B and C), which shows that the miR-21 surge induced by 2/3 PH does not effectively antagonize the expression of PTEN in early liver regeneration. In addition, the finding reveals that accumulation of PTEN does not prevent Akt1 activation in liver regeneration. Viewed together, our results exclude suppression of PTEN by miR-21 as the reason for Akt1 and mTORC1 activation in liver regeneration and confirm our hypothesis that miR-21 facilitates rapid translation of cyclin D1 by relieving Akt1 and its mediator mTORC1 from inhibition by Rhob (Figure 19).

4.3 Discussion

Recently, Rhob was shown to form a ternary complex with the Rho effector kinase (PRK) and the pivotal Akt regulatory kinase PDK1(97). Given the emerging regulatory connections between Rhob and the Akt pathway, Rhob's ability to inhibit Akt1 phosphorylation (98, 99), and the Akt pathway's ability to regulate cap-dependent translation, we postulated that Rhob's effects on cyclin D1 may be a result of it inhibiting the Akt pathway. Overexpression and knockdown of Rhob led to a corresponding decrease and increase in cyclin D1 protein levels thus showing that Rhob can regulate cyclin D1 expression. Since Cyclin D1 translation is mediated by the eIF-4F translation initiation complex, which is activated by Akt1/mTORC1 signaling (34, 92), we decided to examine levels of phosphorylated-Akt1 and phosphorylated-4E-BP1 to determine whether cap-dependent translation of cyclin D1 was affected by Rhob expression. Our data suggests that Rhob can inhibit cyclin D1 translation by antagonizing Akt1/mTOR signaling. Furthermore, loss of cyclin D1 expression caused by miR-21-ASO can be rescued by treatment with siRNAs against Rhob. This result confirmed that miR-21 promotes cyclin D1 translation by inhibiting Rhob and activating mTOR-mediated cap-dependent translation. Finally,

we showed that mice injected with miR-21-ASO after 2/3 PH fail to downregulate Rhob and hence activate Akt/mTOR signaling resulting reduced cyclin D1 expression.

Our finding that miR-21 promotes cyclin D1 translation in liver regeneration by activating Akt1/mTORC1 prompted us to investigate whether PTEN, a miR-21 target known to inhibit Akt1 (53, 96), is also involved in this process. After performing 2/3 PH on normal mice we found that PTEN protein accumulates during G1 phase despite the surge in miR-21 expression induced by 2/3 PH. The finding reveals that accumulation of PTEN does not prevent Akt1 activation in normal liver regeneration. Moreover, the finding shows that suppression of PTEN by miR-21 is not involved in Akt1 activation and thus cyclin D1 translation in early liver regeneration. Nevertheless, viewing miR-21's previously reported ability to activate Akt1 by inhibiting PTEN in cancer cells (53, 96) together with our results suggests the intriguing possibility that miR-21 acts as a central regulator of Akt1/mTORC1 signaling in other contexts.

Figures and Tables

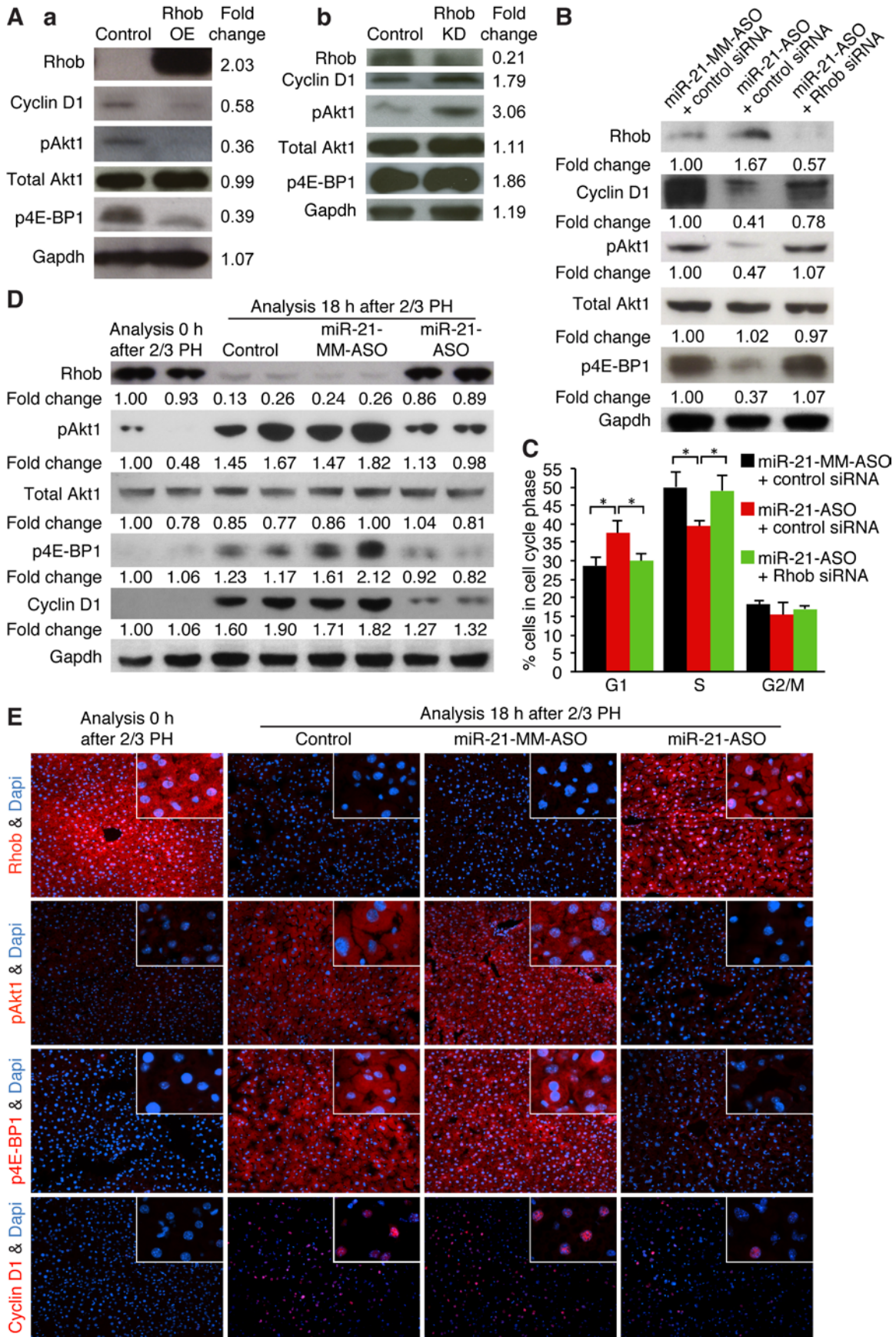


Figure 16 miR-21 promotes cyclin D1 translation in liver regeneration by relieving Akt1-mediated activation of mTORC1 from suppression by Rhob. **(A)** Immunoblotting shows that transfecting a Rhob overexpression (OE) plasmid into Hepa1,6 cells decreases the level of cyclin D1, the level of Akt1 activated by phosphorylation at Ser473 (pAkt1) and the level of 4E-BP1 inhibited by phosphorylation at Thr37 and/or Thr46 (p4E-BP1). Hepa1,6 cells transfected with empty OE plasmid were used as control **(a)**. Rhob knockdown (KD) with a short hairpin RNA (shRNA) plasmid increases the levels of cyclin D1, pAkt1 and p4E-BP1 in Hepa1,6 cells overexpressing Rhob (Control) **(b)**. Numbers indicate protein levels relative to control. Results representative of 3 separate experiments are shown (Supplemental Figure 12A). Gapdh was analyzed as a loading control. **(B)** Immunoblotting shows that miR-21-ASO transfection into Hepa1,6 cells increases Rhob and decreases cyclin D1 levels. This is accompanied by decreased Akt1 and 4E-BP1 phosphorylation. Additional Rhob knockdown with small interfering RNA (siRNA) restores cyclin D1 levels with a corresponding increase in Akt1 and 4E-BP1 phosphorylation. Hepa1,6 cells transfected with miR-21-MM-ASO and non-targeting control siRNA were used as control. Numbers indicate protein levels relative to control. Results representative of 3 separate experiments are shown. Gapdh was analyzed as a loading control. **(C)** Cell cycle analysis was carried out using cells transfected with miR-21-ASO and rescued with Rhob KD. miR-21-MM-ASO and control siRNA were used as controls. Inhibition of miR-21 by miR-21-ASO led to accumulation of cells in G1 phase and a corresponding decrease of cells in S phase. This can be rescued by knocking down Rhob. **(D)** Immunoblotting shows that Rhob levels decrease and pAkt1 and p4E-BP1 levels increase after 2/3 PH in livers of control mice and miR-21-MM-ASO injected mice. Liver samples were obtained by 2/3 PH and 18 hours later. Livers of mice injected with miR-21-ASO show failure to decrease Rhob levels and increase pAkt1 and p4E-BP1 levels at 18 hours after 2/3 PH. Numbers indicate protein levels relative to time point 0 hours after 2/3 PH. Gapdh was analyzed as a loading control. **(E)** Confirmation of the immunoblotting results by immunostaining for Rhob, pAkt1 and p4E-BP1 (all red). At least 3 mice were analyzed for each time point and treatment (Supplemental Figure 12B). miR-21-ASO was injected at 6 hours after 2/3 PH. Control mice were injected with carrier or miR-21-MM-ASO at 6 hours after 2/3 PH.

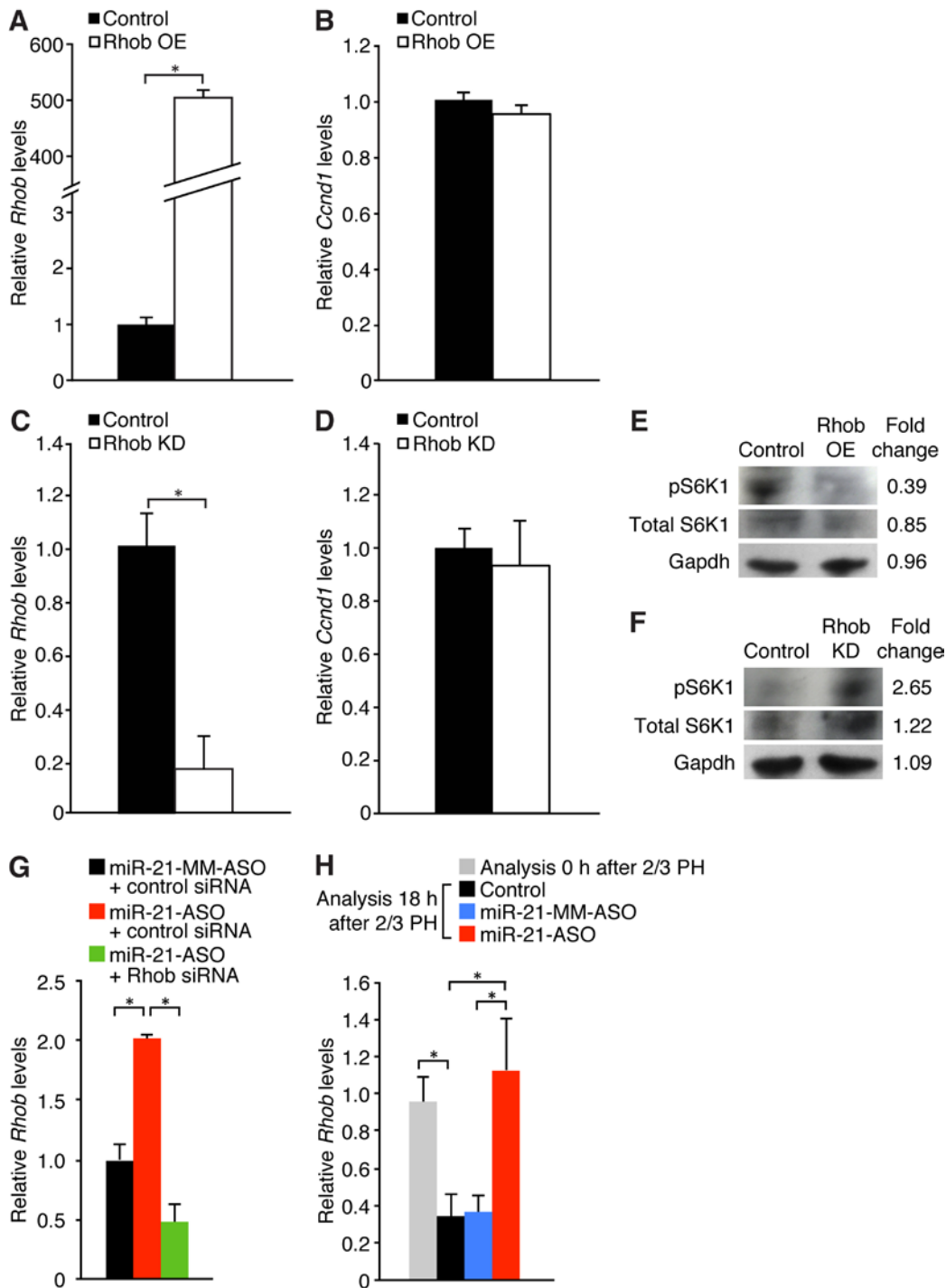


Figure 17 Further evidence that miR-21 promotes cyclin D1 translation by relieving Akt1-mediated activation of mTORC1 from suppression by Rhob. qRT-PCR was used to determine *Rhob* and *Ccnd1* mRNA levels in Hepa1,6 cells transfected with Rhob OE or Rhob OE and KD plasmids. (A) Increased *Rhob* mRNA levels in Hepa1,6 cells transfected with Rhob OE plasmid as compared to cells transfected with empty OE plasmid (Control). (B) Despite Rhob overexpression, *Ccnd1* mRNA levels are unchanged. (C) Decreased *Rhob* mRNA levels in Hepa1,6 cells transfected with both Rhob OE and Rhob KD plasmids (Rhob KD) as compared to cells transfected with Rhob OE plasmid alone (Control).

(D) Despite Rhob knockdown, *Ccnd1* mRNA levels are unchanged. (E) Immunoblotting shows that transfection of Rhob OE plasmid into Hepa1,6 cells decreases the level of S6K1 phosphorylated at Thr389 (pS6K1). Hepa1,6 cells transfected with empty OE plasmid were used as control. (F) Transfection of Rhob KD plasmid into Hepa1,6 cells overexpressing Rhob (Control) increases the level of pS6K1. Numbers indicate protein levels relative to control. Results representative of 3 separate experiments are shown. Gapdh was analyzed as a loading control. (G) qRT-PCR shows that de-repressed *Rhob* mRNA levels in Hepa1,6 cells transfected with miR-21-ASO are normalized after additional transfection of Rhob siRNA. (H) qRT-PCR shows a 3-fold increase in *Rhob* mRNA levels at 18 hours after 2/3 PH in mice injected with miR-21-ASO as compared to control mice. Control mice were injected with carrier at 6 hours after 2/3 PH. At least 3 mice were analyzed for each time point and treatment. Data represent mean \pm SEM. * $P < 0.05$.

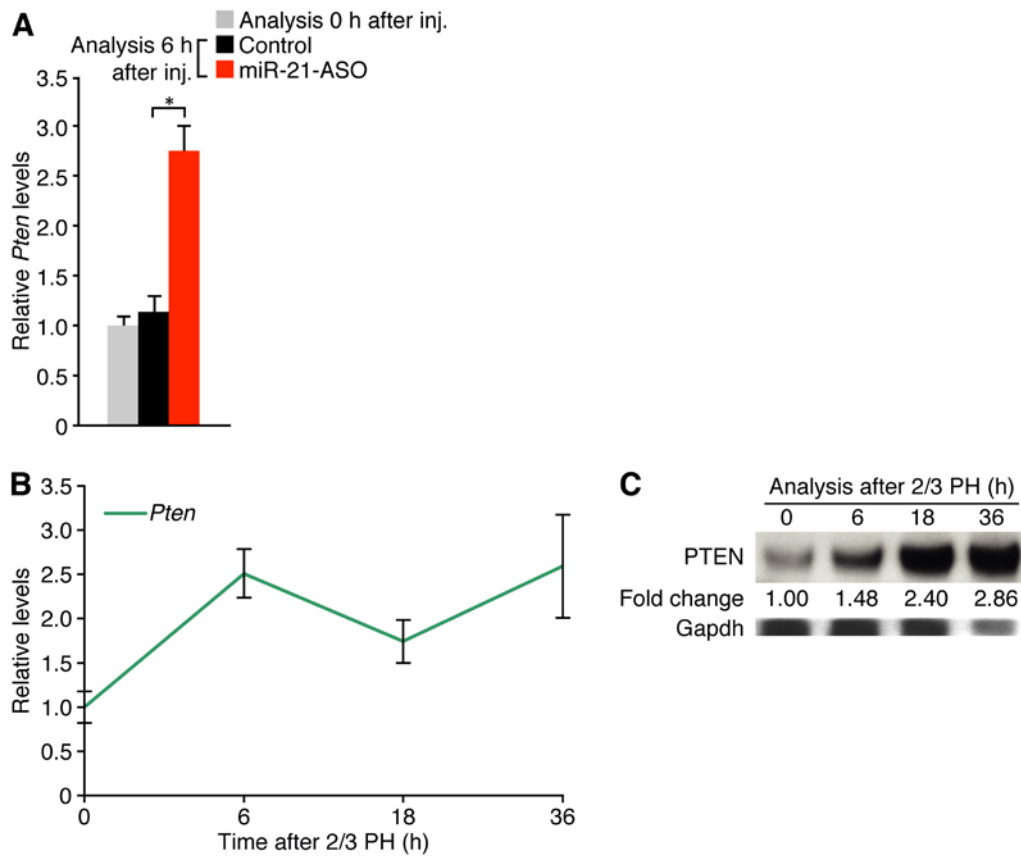


Figure 18 Overexpression of the miR-21 target PTEN in early liver regeneration. **(A)** qRT-PCR shows a 2.5-fold increase in *Pten* mRNA levels in livers of mice 6 hours after a single tail vein injection of miR-21-ASO. Control mice were injected with carrier. **(B)** qRT-PCR shows a rapid and continuous increase in *Pten* mRNA levels after 2/3 PH. **(C)** Immunoblotting shows that PTEN protein levels also increase after 2/3 PH, which excludes effective inhibition by miR-21. Numbers indicate protein levels relative to time point 0 hours after 2/3 PH. Gapdh was analyzed as a loading control. At least 3 mice were analyzed for each time point and treatment. Data represent mean \pm SEM. * $P < 0.05$.

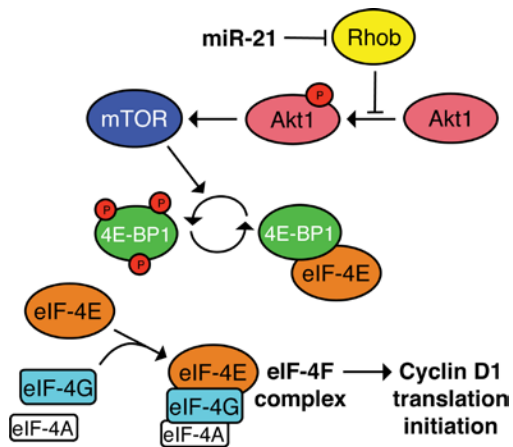


Figure 19 Model of the proposed mechanism of how miR-21 promotes cyclin D1 translation in liver regeneration. By directly inhibiting Rhob expression, miR-21 facilitates Akt1-mediated activation of mTORC1, which promotes cyclin D1 translation initiation. This effect of mTORC1 involves phosphorylation of 4E-BP1, which disables its inhibitory binding of eIF-4E and allows assembly of the eIF-4F complex that additionally contains eIF-4G and eIF-4A (90, 92, 93).

Chapter 5: Conclusions and Future Directions

In conclusion, our results reveal that the increased expression of miR-21 during liver regeneration functions to kick-start cyclin D1 translation in hepatocytes. We found that timing the *in vivo* application of miR-21-ASO so that it antagonized the initial phase of induced miR-21 expression after 2/3 PH prevented cyclin D1 translation in hepatocytes, leading to impaired progression through G1 and into S phase. This effect of miR-21 is mediated by a novel mechanism that integrates inhibition of Rhob by miR-21 with a previously unrecognized function of Rhob, the suppression of eIF-4F-mediated translation initiation through suppression of Akt1/mTORC1 signaling. Viewing our results together with miR-21's ability to activate Akt1 by inhibiting PTEN (53, 96) suggests miR-21 as a key regulator of mTORC1. Moreover, our finding that miR-21 de-represses eIF-4F, which mediates the rate-limiting ribosomal binding step of translation initiation, reveals its profound impact on cell proliferation. Our findings reveal that the induction of miR-21 expression in the early phase of liver regeneration functions to accelerate hepatocyte proliferation by facilitating cyclin D1 translation, a mechanism that may also be effective in other regenerative cell types and cancer cells.

Our finding that miR-21-ASO can be used to partially inhibit miR-21 and de-repress its target genes within 8 hours after intravenous injection has important implications: First, it highlights a method of miRNA inhibition in hepatocytes that avoids unspecific changes due to compensation or adaptation, which can mask or confound the phenotype caused by deficiency of the miRNA. Compensation of impaired hepatocyte proliferation by redundant signaling pathways occurs not instantaneously, but typically within a day after 2/3 PH (20). The rapid onset of miR-21 inhibition by miR-21-ASO limits the time available for activation of redundant pathways and may therefore be more effective for studies of liver regeneration than genetic deletion. In addition, limiting the extent of miRNA inhibition in hepatocytes may help to maintain homeostasis and avoid secondary changes and adaptation. Then, our study shows that the rapid onset of miR-21-ASO's effect allows the dynamic processes that occur

during liver regeneration to be dissected: miR-21 and *Ccnd1* expression are concomitantly induced after 2/3 PH and our results reveal that promotion of cyclin D1 translation is critical for the early phase of liver regeneration when *Ccnd1* mRNA levels are still low, but not for later phases. Finally, our results raise the possibility of using oligonucleotide mimics of miR-21 for therapy of liver failure. Provided that miR-21 mimics enter hepatocytes and exert their function as quickly as miR-21-ASO, they may be effective in accelerating progression of hepatocytes through G1 and into S phase, which is critical for survival from liver injury (100).

Chapter 6: Materials and Methods

miR-21-ASO and miR-21-MM-ASO generation

Both oligonucleotides were produced by Exiqon. To prevent toxicity and facilitate efficient cellular uptake, a short (< 16mer) design was chosen. Both oligonucleotides had a fully phosphorothioate-modified backbone. The sequence of miR-21-ASO is TCAGTCTGATAAGCT. High target affinity was ensured by LNA modifications. miR-21-MM-ASO is identical to miR-21-ASO, except for 4 base-pair changes that prevent binding to miR-21. Its sequence is TCAGTATTAGCAGCT. Both oligonucleotides were purified by reverse-phase high performance liquid chromatography and lyophilized.

miR-21-ASO and miR-21-MM-ASO intravenous injection

Lyophilized oligonucleotide was resuspended in NaCl 0.9% to a final concentration of 30 $\mu\text{g}/\mu\text{l}$. A dose of 25 $\mu\text{g}/\text{g}$ body weight oligonucleotide in a total volume of 100 μl NaCl 0.9% was injected via the tail vein into 8 to 12-week-old male C57BL/6 mice (Jackson Laboratory). Control mice were injected with 100 μl NaCl 0.9% (carrier). All procedures involving mice were approved by the Institutional Animal Care and Use Committee at UCSF.

2/3 partial hepatectomy

Two-thirds of the liver was surgically removed under isoflurane anesthesia as previously described (3).

BrdU labeling

50 µg/g body weight BrdU (Roche) dissolved in PBS were injected intraperitoneally 2 hours before the mice were killed for analysis.

Quantitative Real-Time PCR

Total RNA was isolated with the miRNAeasy kit (Qiagen) and treated with DNase I (Ambion) to eliminate genomic DNA. Superscript III reverse transcription reagent (Invitrogen) was used to generate cDNA using 1 µg of total RNA. PCR amplification was performed as previously described (55). Primers for qRT-PCR were designed using Beacon Designer (Premier Biosoft). miRNA isolation, amplification and analysis were performed as previously described including normalization to sno202RNA (55). Relative changes in mRNA and miRNA expression were determined using the 2- $\Delta\Delta$ Ct method(101).

Immunostaining

Paraffin-embedded liver samples were sectioned and stained with the antibodies rabbit anti-cyclin D1 (NeoMarkers), mouse anti-PCNA (Biosource) and rabbit anti-Ki67 (Lab Vision) at 1:100 dilutions. Immunostainings of sections of frozen liver samples embedded in optimum cutting temperature compound (Tissue-Tek, Sakura Finetek) were performed with rabbit anti-RhoB (Santa Cruz Biotechnology), rabbit anti-Akt1 phosphorylated at Ser473, rabbit anti-4E-BP1 phosphorylated at Thr37 and/or Thr46 (both Cell Signaling), rat anti-BrdU (Abcam) and

rabbit anti-cyclin D1 (Neomarkers) antibodies at 1:100 dilutions. For fluorescence microscopy, the secondary antibody goat anti-rabbit conjugated with Alexa Fluor 594 (Invitrogen) and goat anti-rat conjugated with Alexa Fluor 594 (Invitrogen) was used at 1:500 dilutions. Nuclear DNA was stained with 300 nM Dapi (Millipore).

Immunoblotting

Liver samples were immediately frozen in liquid nitrogen and homogenized in 20 mM Tris buffer, pH 7.4, containing 150 mM NaCl, 1% Triton X-100, 10 mM EDTA and Complete Protease Inhibitor Cocktail (Roche Applied Science). After homogenization, tissue extracts were centrifuged at 14,000 x g at 4°C and supernatants were collected. Protein concentration was measured using the Bradford assay (Biorad). 50 µg of protein per well was loaded on 13% sodium dodecyl sulfate-polyacrylamide gels. After electrophoresis, gels were electrotransferred onto polyvinylidene fluoride membranes (Biorad). Membranes were blocked with 5% bovine serum albumin (BSA) in Tris-buffered saline with 0.1% Tween 20 (Sigma; TBST) and incubated with primary antibodies in 5% BSA in TBST. In addition to the antibodies listed above, rabbit anti-RhoB, rabbit anti-Akt1, rabbit anti-Gsk3b, rabbit anti-Gsk3b phosphorylated at Ser9, rabbit anti-PTEN, rabbit anti-Pdc4, rabbit anti-S6K1 and rabbit anti-S6K1 phosphorylated at Thr389 and rabbit anti-Gapdh (all Cell Signaling) antibodies were used. After 3 washes with TBST, membranes were incubated with the secondary antibody goat anti-rabbit-HRP (Jackson ImmunoResearch) at 1:10,000 dilutions in 5% BSA in TBST and developed with ECL or ECLplus Western Chemiluminescent HRP substrate (Pierce). Signal intensities were quantified and normalized to Gapdh using ImageJ.

Ccnd1-ASO generation and intravenous injection

The *Ccnd1*-ASO was produced by Isis Pharmaceuticals. The 20mer was stabilized by replacing oxygen with sulphur throughout the backbone and making methoxyethyl modifications on the 2' position of the sugar of the first 5 nucleotides at the 5' and 3' end. Lyophilized *Ccnd1*-ASO and a non-targeting control ASO (NT-ASO) were resuspended in NaCl 0.9% to a final concentration of 20 µg/µl. A dose of 50 µg/g body weight ASO in a total volume of 100 µl NaCl 0.9% was injected via the tail vein into 8 to 12-week-old male C57BL/6 mice (Jackson Laboratory).

miRNA mimic and inhibitor transfection

miR-21 mimic or hairpin inhibitor (both Dharmacon), miR-21-ASO or miR-21-MM-ASO was introduced into Hepa1,6 cells at a final concentration of 20, 40 or 80 nM. Hepa1,6 cells were plated in 24-well plates (Corning; 5 x 10⁴ cells/well) and transfected 24 hours later using Lipofectamine 2000 (Invitrogen). Equal concentrations of double-stranded or single-stranded oligonucleotide sense or antisense to cel-miR-67 were used as non-targeting controls for miR-21 mimic or inhibitor, respectively.

Polysome analysis

Isolation and analysis of polysomal fractions was performed as previously described (13) with some modifications. Hepa1,6 cells (ATCC) were seeded into 15 cm tissue culture plates and transfected at 50% confluency with 40 nM miR-21-ASO using Lipofectamine 2000 and harvested 48 hours later. Control cells were transfected with 40 nM non-targeting ASO. Cells were lysed in ice-cold buffer A (10 mM Tris-HCl pH 8, 140 mM NaCl, 1.5 mM MgCl₂, 0.25%

NP-40, 0.5% Triton X-100 supplemented with 40 U/ml RNase inhibitor (Promega), 150 µg/ml cycloheximide and 20mM dithiothreitol) for 40 minutes on ice. Lysates were centrifuged at 10,000 x g for 10 minutes at 4°C and supernatants of equal volume were loaded onto 10-60% sucrose gradients in buffer B (25 mM Tris-HCl, 25 mM NaCl and 1.5 mM MgCl₂). Sucrose density gradient centrifugation was carried out at 100,000 x g for 3 hours at 4°C using an SW41Ti rotor (Beckman). Fractions were collected using an ISCO gradient fraction collector. RNA from each fraction and unfractionated samples was isolated using Trizol (Invitrogen), purified using Purelink RNA mini kit (Invitrogen) and treated with Turbo DNase (Ambion) before reverse transcription. *Ccnd1* mRNA levels in fractionated and unfractionated RNA were determined by qRT-PCR and were normalized to *Gapdh* expression. To account for potential variations in overall *Ccnd1* mRNA levels between samples caused by differences in cell numbers, *Ccnd1* mRNA levels of fractionated RNA were further normalized to *Ccnd1* mRNA levels of the respective unfractionated RNA. Unless specified, reagents were from Sigma.

Rhob overexpression

Rhob cDNA was amplified from mouse liver total RNA and cloned into pIRES-GFP (Clontech) to generate the Rhob OE plasmid. Hepa1,6 cells were plated in 6-well plates (Corning; 5 x 10⁵ cells/well) and transfected 24 hours later with 3 µg Rhob OE plasmid using Lipofectamine 2000. Rhob expression was determined using qRT-PCR and immunoblotting 48 hours later.

Rhob inhibition

shRNA sequences for mouse *Rhob* were designed using the Hush-27 algorithm (Origene) and cloned into pGFP-V-RS (Origene). Hepa1,6 cells were plated in 6-well plates (5×10^5 cells/well) and transfected 24 hours later with 2 μg pGFP-V-RS containing *Rhob*-shRNA and 2 μg Rhob OE plasmid using Fugene HD (Roche). Cells were collected 72 hours later and Rhob expression was analyzed using qRT-PCR and immunoblotting. To determine the consequences of knockdown of both miR-21 and Rhob, Hepa1,6 cells were plated in 6-well plates (5×10^5 cells/well) and transfected 24 hours later with miR-21-ASO and Rhob siRNA or negative control siRNA (both Qiagen) at a final concentration of 40 and 10 nM, respectively. Cells transfected with miR-21-MM-ASO and negative control siRNA at 40 and 10 nM final concentrations were used as control. Cells were collected 24 hours later for analysis by qRT-PCR and immunoblotting.

Luciferase assay

Rhob 3' UTR was amplified from mouse genomic DNA and cloned into the pMIR-REPORT vector (Ambion). To generate the mutant *Rhob* 3' UTR, mutations were introduced into the sequence complementary to the miR-21 seed sequence using the QuickChange Site-directed Mutagenesis Kit (Stratagene). Constructs were validated by sequencing. Hepa1,6 cells were plated in 24-well plates (5×10^4 cells/well) and transfected 24 hours later with miR-21 mimic or inhibitor and 30 ng of the pMIRREPORT vector containing the wildtype or mutant *Rhob* 3' UTR and 30 ng of the pSV- β -Galactosidase Control Vector (Promega) to monitor transfection efficiencies. 24 hours after transfection, luciferase and β -galactosidase activities were

measured using the Luciferase Assay System and Beta-Glo Assay System (both Promega) in a Synergy 2 Microplate Reader (BioTek Instruments). Luciferase activities were normalized to β -galactosidase activities for each well.

Cell cycle phase distribution analysis

Hep1,6 cells were plated in 6-well plates (1×10^6 cells/well) and cultured for 24 hours before the indicated oligonucleotides were transfected at the same final concentrations as for immunoblotting. 24 hours after transfection, cells were fixed by incubation in ice-cold 70% ethanol for at least 16 hours. After fixation, 2×10^5 cells were stained in 10 μ g/ml propidium iodide (Sigma) for 30 minutes at room temperature in the dark. Flow cytometry was performed on a LSR II and data was analyzed by CellQuest software (both BD Biosciences).

Data analysis

Statistical significance was determined with two-tailed Student's *t*-tests. $P < 0.05$ was considered significant.

References

1. Michalopoulos, G.K. 2007. Liver regeneration. *J Cell Physiol* 213:286-300.
2. Higgins GM, A.R. 1931. Experimental Pathology of the liver, I: Restoration of the liver of the white rat following partial surgical removal. *Arch Pathol* 12:186-202.
3. Mitchell, C., and Willenbring, H. 2008. A reproducible and well-tolerated method for 2/3 partial hepatectomy in mice. *Nat Protoc* 3:1167-1170.
4. Juskeviciute, E., Vadigepalli, R., and Hoek, J.B. 2008. Temporal and functional profile of the transcriptional regulatory network in the early regenerative response to partial hepatectomy in the rat. *BMC Genomics* 9:527.
5. Rabes, H.M. 1977. Kinetics of hepatocellular proliferation as a function of the microvascular structure and functional state of the liver. *Ciba Found Symp*:31-53.
6. Gebhardt, R., Baldysiak-Figiel, A., Krugel, V., Ueberham, E., and Gaunitz, F. 2007. Hepatocellular expression of glutamine synthetase: an indicator of morphogen actions as master regulators of zonation in adult liver. *Prog Histochem Cytochem* 41:201-266.
7. Fausto, N., Campbell, J.S., and Riehle, K.J. 2006. Liver regeneration. *Hepatology* 43:S45-53.
8. Fausto, N. 1999. Lessons from genetically engineered animal models. V. Knocking out genes to study liver regeneration: present and future. *Am J Physiol* 277:G917-921.
9. Webber, E.M., Bruix, J., Pierce, R.H., and Fausto, N. 1998. Tumor necrosis factor primes hepatocytes for DNA replication in the rat. *Hepatology* 28:1226-1234.
10. Mars, W.M., Liu, M.L., Kitson, R.P., Goldfarb, R.H., Gabauer, M.K., and Michalopoulos, G.K. 1995. Immediate early detection of urokinase receptor after partial hepatectomy and its implications for initiation of liver regeneration. *Hepatology* 21:1695-1701.
11. Mars, W.M., Kim, T.H., Stolz, D.B., Liu, M.L., and Michalopoulos, G.K. 1996. Presence of urokinase in serum-free primary rat hepatocyte cultures and its role in activating hepatocyte growth factor. *Cancer Res* 56:2837-2843.
12. Pardee, A.B. 1989. G1 events and regulation of cell proliferation. *Science* 246:603-608.
13. Albrecht, J.H., and Hansen, L.K. 1999. Cyclin D1 promotes mitogen-independent cell cycle progression in hepatocytes. *Cell Growth Differ* 10:397-404.
14. Nelsen, C.J., Rickheim, D.G., Timchenko, N.A., Stanley, M.W., and Albrecht, J.H. 2001. Transient expression of cyclin D1 is sufficient to promote hepatocyte replication and liver growth in vivo. *Cancer Res* 61:8564-8568.
15. Sherr, C.J. 2000. The Pezcoller lecture: cancer cell cycles revisited. *Cancer Res* 60:3689-3695.
16. Sherr, C.J., and Roberts, J.M. 1999. CDK inhibitors: positive and negative regulators of G1-phase progression. *Genes Dev* 13:1501-1512.
17. Nelsen, C.J., Rickheim, D.G., Tucker, M.M., Hansen, L.K., and Albrecht, J.H. 2003. Evidence that cyclin D1 mediates both growth and proliferation downstream of TOR in hepatocytes. *J Biol Chem* 278:3656-3663.
18. Mullany, L.K., White, P., Hanse, E.A., Nelsen, C.J., Goggin, M.M., Mullany, J.E., Anttila, C.K., Greenbaum, L.E., Kaestner, K.H., and Albrecht, J.H. 2008. Distinct proliferative and transcriptional effects of the D-type cyclins in vivo. *Cell Cycle* 7:2215-2224.
19. Fausto, N., and Riehle, K.J. 2005. Mechanisms of liver regeneration and their clinical implications. *J Hepatobiliary Pancreat Surg* 12:181-189.
20. Michalopoulos, G.K. 2010. Liver regeneration after partial hepatectomy: critical analysis of mechanistic dilemmas. *Am J Pathol* 176:2-13.
21. Mawet, E., Shiratori, Y., Hikiba, Y., Takada, H., Yoshida, H., Okano, K., Komatsu, Y., Matsumura, M., Niwa, Y., and Omata, M. 1996. Cytokine-induced neutrophil chemoattractant release from hepatocytes is modulated by Kupffer cells. *Hepatology* 23:353-358.

22. Koniaris, L.G., McKillop, I.H., Schwartz, S.I., and Zimmers, T.A. 2003. Liver regeneration. *J Am Coll Surg* 197:634-659.
23. Borowiak, M., Garratt, A.N., Wustefeld, T., Strehle, M., Trautwein, C., and Birchmeier, C. 2004. Met provides essential signals for liver regeneration. *Proc Natl Acad Sci U S A* 101:10608-10613.
24. Jackson, L.N., Larson, S.D., Silva, S.R., Rychahou, P.G., Chen, L.A., Qiu, S., Rajaraman, S., and Evers, B.M. 2008. PI3K/Akt activation is critical for early hepatic regeneration after partial hepatectomy. *Am J Physiol Gastrointest Liver Physiol* 294:G1401-1410.
25. Haga, S., Ozaki, M., Inoue, H., Okamoto, Y., Ogawa, W., Takeda, K., Akira, S., and Todo, S. 2009. The survival pathways phosphatidylinositol-3 kinase (PI3-K)/phosphoinositide-dependent protein kinase 1 (PDK1)/Akt modulate liver regeneration through hepatocyte size rather than proliferation. *Hepatology* 49:204-214.
26. Hong, F., Nguyen, V.A., Shen, X., Kunos, G., and Gao, B. 2000. Rapid activation of protein kinase B/Akt has a key role in antiapoptotic signaling during liver regeneration. *Biochem Biophys Res Commun* 279:974-979.
27. Gao, T., Furnari, F., and Newton, A.C. 2005. PHLPP: a phosphatase that directly dephosphorylates Akt, promotes apoptosis, and suppresses tumor growth. *Mol Cell* 18:13-24.
28. Sarbassov, D.D., Ali, S.M., Kim, D.H., Guertin, D.A., Latek, R.R., Erdjument-Bromage, H., Tempst, P., and Sabatini, D.M. 2004. Rictor, a novel binding partner of mTOR, defines a rapamycin-insensitive and raptor-independent pathway that regulates the cytoskeleton. *Curr Biol* 14:1296-1302.
29. Bellacosa, A., Kumar, C.C., Di Cristofano, A., and Testa, J.R. 2005. Activation of AKT kinases in cancer: implications for therapeutic targeting. *Adv Cancer Res* 94:29-86.
30. Vivanco, I., and Sawyers, C.L. 2002. The phosphatidylinositol 3-Kinase AKT pathway in human cancer. *Nat Rev Cancer* 2:489-501.
31. Watanabe, H., Saito, H., Rychahou, P.G., Uchida, T., and Evers, B.M. 2005. Aging is associated with decreased pancreatic acinar cell regeneration and phosphatidylinositol 3-kinase/Akt activation. *Gastroenterology* 128:1391-1404.
32. Bjornsti, M.A., and Houghton, P.J. 2004. Lost in translation: dysregulation of cap-dependent translation and cancer. *Cancer Cell* 5:519-523.
33. Hay, N., and Sonenberg, N. 2004. Upstream and downstream of mTOR. *Genes Dev* 18:1926-1945.
34. Fingar, D.C., Richardson, C.J., Tee, A.R., Cheatham, L., Tsou, C., and Blenis, J. 2004. mTOR controls cell cycle progression through its cell growth effectors S6K1 and 4E-BP1/eukaryotic translation initiation factor 4E. *Mol Cell Biol* 24:200-216.
35. Ambros, V. 2001. microRNAs: tiny regulators with great potential. *Cell* 107:823-826.
36. Ambros, V. 2003. MicroRNA pathways in flies and worms: growth, death, fat, stress, and timing. *Cell* 113:673-676.
37. Borchert, G.M., Lanier, W., and Davidson, B.L. 2006. RNA polymerase III transcribes human microRNAs. *Nat Struct Mol Biol* 13:1097-1101.
38. Cai, X., Hagedorn, C.H., and Cullen, B.R. 2004. Human microRNAs are processed from capped, polyadenylated transcripts that can also function as mRNAs. *RNA* 10:1957-1966.
39. Lee, Y., Kim, M., Han, J., Yeom, K.H., Lee, S., Baek, S.H., and Kim, V.N. 2004. MicroRNA genes are transcribed by RNA polymerase II. *EMBO J* 23:4051-4060.
40. Lee, Y., Ahn, C., Han, J., Choi, H., Kim, J., Yim, J., Lee, J., Provost, P., Radmark, O., Kim, S., et al. 2003. The nuclear RNase III Drosha initiates microRNA processing. *Nature* 425:415-419.
41. Bohnsack, M.T., Czaplinski, K., and Gorlich, D. 2004. Exportin 5 is a RanGTP-dependent dsRNA-binding protein that mediates nuclear export of pre-miRNAs. *RNA* 10:185-191.
42. Lund, E., Guttinger, S., Calado, A., Dahlberg, J.E., and Kutay, U. 2004. Nuclear export of microRNA precursors. *Science* 303:95-98.
43. Yi, R., Doehle, B.P., Qin, Y., Macara, I.G., and Cullen, B.R. 2005. Overexpression of exportin 5 enhances RNA interference mediated by short hairpin RNAs and microRNAs. *RNA* 11:220-226.

44. Brennecke, J., Stark, A., Russell, R.B., and Cohen, S.M. 2005. Principles of microRNA-target recognition. *PLoS Biol* 3:e85.
45. Krol, J., Loedige, I., and Filipowicz, W. 2010. The widespread regulation of microRNA biogenesis, function and decay. *Nat Rev Genet* 11:597-610.
46. Krichevsky, A.M., and Gabriely, G. 2009. miR-21: a small multi-faceted RNA. *J Cell Mol Med* 13:39-53.
47. Chan, J.A., Krichevsky, A.M., and Kosik, K.S. 2005. MicroRNA-21 is an antiapoptotic factor in human glioblastoma cells. *Cancer Res* 65:6029-6033.
48. Selcuklu, S.D., Donoghue, M.T., and Spillane, C. 2009. miR-21 as a key regulator of oncogenic processes. *Biochem Soc Trans* 37:918-925.
49. Garzon, R., Marcucci, G., and Croce, C.M. 2010. Targeting microRNAs in cancer: rationale, strategies and challenges. *Nat Rev Drug Discov* 9:775-789.
50. Connolly, E.C., Van Doorslaer, K., Rogler, L.E., and Rogler, C.E. 2010. Overexpression of miR-21 promotes an in vitro metastatic phenotype by targeting the tumor suppressor RHOB. *Mol Cancer Res* 8:691-700.
51. Fujita, S., Ito, T., Mizutani, T., Minoguchi, S., Yamamichi, N., Sakurai, K., and Iba, H. 2008. miR-21 Gene expression triggered by AP-1 is sustained through a double-negative feedback mechanism. *J Mol Biol* 378:492-504.
52. Loffler, D., Brocke-Heidrich, K., Pfeifer, G., Stocsits, C., Hackermuller, J., Kretzschmar, A.K., Burger, R., Gramatzki, M., Blumert, C., Bauer, K., et al. 2007. Interleukin-6 dependent survival of multiple myeloma cells involves the Stat3-mediated induction of microRNA-21 through a highly conserved enhancer. *Blood* 110:1330-1333.
53. Meng, F., Henson, R., Wehbe-Janek, H., Ghoshal, K., Jacob, S.T., and Patel, T. 2007. MicroRNA-21 regulates expression of the PTEN tumor suppressor gene in human hepatocellular cancer. *Gastroenterology* 133:647-658.
54. Frankel, L.B., Christoffersen, N.R., Jacobsen, A., Lindow, M., Krogh, A., and Lund, A.H. 2008. Programmed cell death 4 (PDCD4) is an important functional target of the microRNA miR-21 in breast cancer cells. *J Biol Chem* 283:1026-1033.
55. Song, G., Sharma, A.D., Roll, G.R., Ng, R., Lee, A.Y., Blemlock, R.H., Frandsen, N.M., and Willenbring, H. 2010. MicroRNAs control hepatocyte proliferation during liver regeneration. *Hepatology* 51:1735-1743.
56. Song, G., Sharma, A., Roll, G., Ng, R., Lee, A., Blemlock, R., Frandsen, N., and Willenbring, H. 2010. MicroRNAs control hepatocyte proliferation during liver regeneration. *Hepatology* 51:1735-1743.
57. Marquez, R.T., Wendlandt, E., Galle, C.S., Keck, K., and McCaffrey, A.P. 2010. MicroRNA-21 is upregulated during the proliferative phase of liver regeneration, targets Pellino-1, and inhibits NF-kappaB signaling. *Am J Physiol Gastrointest Liver Physiol* 298:G535-541.
58. Castro, R.E., Ferreira, D.M., Zhang, X., Borralho, P.M., Sarver, A.L., Zeng, Y., Steer, C.J., Kren, B.T., and Rodrigues, C.M. 2010. Identification of microRNAs during rat liver regeneration after partial hepatectomy and modulation by ursodeoxycholic acid. *Am J Physiol Gastrointest Liver Physiol* 299:G887-897.
59. Koshkin, A., Singh, S., Nielsen, P., Rajwanshi, V., Kumar, R., Meldgaard, M., Olsen, C., and Wengel, J. 1998. LNA (locked nucleic acids): synthesis of the adenine, cytosine, guanine, 5-methylcytosine, thymine and uracil bicyclonucleoside monomers, oligomerisation, and unprecedented nucleic acid recognition. *Tetrahedron* 54:3607-3630.
60. Elmèn, J., Lindow, M., Sch,tz, S., Lawrence, M., Petri, A., Obad, S., Lindholm, M., Hedtj%orn, M., Hansen, H., and Berger, U. 2008. LNA-mediated microRNA silencing in non-human primates. *Nature* 452:896-899.
61. Elmen, J., Lindow, M., Schutz, S., Lawrence, M., Petri, A., Obad, S., Lindholm, M., Hedtjarn, M., Hansen, H.F., Berger, U., et al. 2008. LNA-mediated microRNA silencing in non-human primates. *Nature* 452:896-899.
62. Elmen, J., Lindow, M., Silaharoglu, A., Bak, M., Christensen, M., Lind-Thomsen, A., Hedtjarn, M., Hansen, J.B., Hansen, H.F., Straarup, E.M., et al. 2008. Antagonism of

- microRNA-122 in mice by systemically administered LNA-antimiR leads to up-regulation of a large set of predicted target mRNAs in the liver. *Nucleic Acids Res* 36:1153-1162.
63. Alao, J.P. 2007. The regulation of cyclin D1 degradation: roles in cancer development and the potential for therapeutic invention. *Mol Cancer* 6:24.
 64. Bellodi, C., Kopmar, N., and Ruggero, D. 2010. Deregulation of oncogene-induced senescence and p53 translational control in X-linked dyskeratosis congenita. *EMBO J* 29:1865-1876.
 65. Ledda-Columbano, G.M., Pibiri, M., Concas, D., Cossu, C., Tripodi, M., and Columbano, A. 2002. Loss of cyclin D1 does not inhibit the proliferative response of mouse liver to mitogenic stimuli. *Hepatology* 36:1098-1105.
 66. Marquez, R.T., Wendlandt, E., Galle, C.S., Keck, K., and McCaffrey, A.P. 2010. MicroRNA-21 is upregulated during the proliferative phase of liver regeneration, targets Pellino-1, and inhibits NF-kappaB signaling. *Am J Physiol Gastrointest Liver Physiol* 298:535-541.
 67. Castro, R.E., Ferreira, D.M., Zhang, X., Borralho, P.M., Sarver, A.L., Zeng, Y., Steer, C.J., Kren, B.T., and Rodrigues, C.M. 2010. Identification of microRNAs during rat liver regeneration after partial hepatectomy and modulation by ursodeoxycholic acid. *Am J Physiol Gastrointest Liver Physiol* 299:887-897.
 68. Rehmsmeier, M., Steffen, P., Hochsmann, M., and Giegerich, R. 2004. Fast and effective prediction of microRNA/target duplexes. *RNA* 10:1507-1517.
 69. Zhang, Y., and Verbeek, F.J. 2010. Comparison and integration of target prediction algorithms for microRNA studies. *J Integr Bioinform* 7.
 70. Witkos, T.M., Koscianska, E., and Krzyzosiak, W.J. 2011. Practical Aspects of microRNA Target Prediction. *Curr Mol Med* 11:93-109.
 71. Alexiou, P., Maragkakis, M., Papadopoulos, G.L., Reczko, M., and Hatzigeorgiou, A.G. 2009. Lost in translation: an assessment and perspective for computational microRNA target identification. *Bioinformatics* 25:3049-3055.
 72. Kiriakidou, M., Nelson, P.T., Kouranov, A., Fitziev, P., Bouyioukos, C., Mourelatos, Z., and Hatzigeorgiou, A. 2004. A combined computational-experimental approach predicts human microRNA targets. *Genes Dev* 18:1165-1178.
 73. Vasudevan, S., Tong, Y., and Steitz, J.A. 2007. Switching from repression to activation: microRNAs can up-regulate translation. *Science* 318:1931-1934.
 74. Orom, U.A., Nielsen, F.C., and Lund, A.H. 2008. MicroRNA-10a binds the 5'UTR of ribosomal protein mRNAs and enhances their translation. *Mol Cell* 30:460-471.
 75. Reimand, J., Kull, M., Peterson, H., Hansen, J., and Vilo, J. 2007. g:Profiler--a web-based toolset for functional profiling of gene lists from large-scale experiments. *Nucleic Acids Res* 35:W193-200.
 76. Goke, R., Barth, P., Schmidt, A., Samans, B., and Lankat-Buttgereit, B. 2004. Programmed cell death protein 4 suppresses CDK1/cdc2 via induction of p21(Waf1/Cip1). *Am J Physiol Cell Physiol* 287:C1541-1546.
 77. Karlsson, R., Pedersen, E.D., Wang, Z., and Brakebusch, C. 2009. Rho GTPase function in tumorigenesis. *Biochim Biophys Acta* 1796:91-98.
 78. Lim, L., Manser, E., Leung, T., and Hall, C. 2004. Regulation of phosphorylation pathways by p21 GTPases. *European Journal of Biochemistry* 242:171-185.
 79. Van Aelst, L., and DiSouza-Schorey, C. 1997. Rho GTPases and signaling networks. *Genes & development* 11:2295.
 80. Connolly, E., Van Doorslaer, K., Rogler, L., and Rogler, C. 2010. Overexpression of miR-21 Promotes an In vitro Metastatic Phenotype by Targeting the Tumor Suppressor RHOB. *Molecular Cancer Research* 8:691.
 81. Aspenstrom, P. 1999. Effectors for the Rho GTPases. *Curr Opin Cell Biol* 11:95-102.
 82. Van Aelst, L., and D'Souza-Schorey, C. 1997. Rho GTPases and signaling networks. *Genes Dev* 11:2295-2322.
 83. Wheeler, A.P., and Ridley, A.J. 2004. Why three Rho proteins? RhoA, RhoB, RhoC, and cell motility. *Exp Cell Res* 301:43-49.

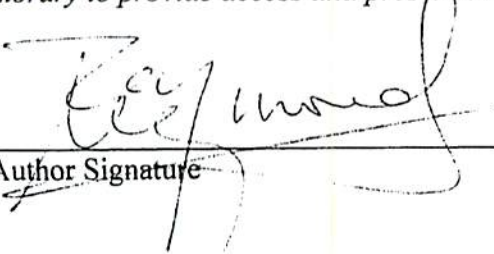
84. Gampel, A., Parker, P.J., and Mellor, H. 1999. Regulation of epidermal growth factor receptor traffic by the small GTPase rhoB. *Curr Biol* 9:955-958.
85. Fritz, G., and Kaina, B. 1997. rhoB encoding a UV-inducible Ras-related small GTP-binding protein is regulated by GTPases of the Rho family and independent of JNK, ERK, and p38 MAP kinase. *J Biol Chem* 272:30637-30644.
86. Fritz, G., Kaina, B., and Aktories, K. 1995. The ras-related small GTP-binding protein RhoB is immediate-early inducible by DNA damaging treatments. *J Biol Chem* 270:25172-25177.
87. Prendergast, G.C. 2001. Actin' up: RhoB in cancer and apoptosis. *Nat Rev Cancer* 1:162-168.
88. Zalzman, G., Closson, V., Linares-Cruz, G., Lerebours, F., Honore, N., Tavitian, A., and Olofsson, B. 1995. Regulation of Ras-related RhoB protein expression during the cell cycle. *Oncogene* 10:1935-1945.
89. Jiang, K., Sun, J., Cheng, J., Djeu, J.Y., Wei, S., and Sebt, S. 2004. Akt mediates Ras downregulation of RhoB, a suppressor of transformation, invasion, and metastasis. *Mol Cell Biol* 24:5565-5576.
90. Flynn, P., Mellor, H., Casamassima, A., and Parker, P.J. 2000. Rho GTPase control of protein kinase C-related protein kinase activation by 3-phosphoinositide-dependent protein kinase. *J Biol Chem* 275:11064-11070.
91. Bousquet, E., Mazieres, J., Privat, M., Rizzati, V., Casanova, A., Ledoux, A., Mery, E., Couderc, B., Favre, G., and Pradines, A. 2009. Loss of RhoB expression promotes migration and invasion of human bronchial cells via activation of AKT1. *Cancer Res* 69:6092-6099.
92. Gingras, A.C., Kennedy, S.G., O'Leary, M.A., Sonenberg, N., and Hay, N. 1998. 4E-BP1, a repressor of mRNA translation, is phosphorylated and inactivated by the Akt(PKB) signaling pathway. *Genes Dev* 12:502-513.
93. Gera, J.F., Mellinghoff, I.K., Shi, Y., Rettig, M.B., Tran, C., Hsu, J.H., Sawyers, C.L., and Lichtenstein, A.K. 2004. AKT activity determines sensitivity to mammalian target of rapamycin (mTOR) inhibitors by regulating cyclin D1 and c-myc expression. *J Biol Chem* 279:2737-2746.
94. Goggin, M.M., Nelsen, C.J., Kimball, S.R., Jefferson, L.S., Morley, S.J., and Albrecht, J.H. 2004. Rapamycin-sensitive induction of eukaryotic initiation factor 4F in regenerating mouse liver. *Hepatology* 40:537-544.
95. Jackson, L.N., Larson, S.D., Silva, S.R., Rychahou, P.G., Chen, L.A., Qiu, S., Rajaraman, S., and Evers, B.M. 2008. PI3K/Akt activation is critical for early hepatic regeneration after partial hepatectomy. *Am J Physiol Gastrointest Liver Physiol* 294:1401-1410.
96. Iliopoulos, D., Jaeger, S.A., Hirsch, H.A., Bulyk, M.L., and Struhl, K. 2010. STAT3 activation of miR-21 and miR-181b-1 via PTEN and CYLD are part of the epigenetic switch linking inflammation to cancer. *Mol Cell* 39:493-506.
97. Flynn, P., Mellor, H., Casamassima, A., and Parker, P. 2000. Rho GTPase control of protein kinase C-related protein kinase activation by 3-phosphoinositide-dependent protein kinase. *Journal of Biological Chemistry* 275:11064.
98. Jackson, L., Larson, S., Silva, S., Rychahou, P., Chen, L., Qiu, S., Rajaraman, S., and Evers, B. 2008. PI3K/Akt activation is critical for early hepatic regeneration after partial hepatectomy. *American Journal of Physiology- Gastrointestinal and Liver Physiology* 294:G1401.
99. Haga, S., Ogawa, W., Inoue, H., Terui, K., Ogino, T., Igarashi, R., Takeda, K., Akira, S., Enosawa, S., and Furukawa, H. 2005. Compensatory recovery of liver mass by Akt-mediated hepatocellular hypertrophy in liver-specific STAT3-deficient mice. *Journal of hepatology* 43:799-807.
100. Clavien, P.A., Petrowsky, H., DeOliveira, M.L., and Graf, R. 2007. Strategies for safer liver surgery and partial liver transplantation. *N Engl J Med* 356:1545-1559.
101. Schmittgen, T.D., and Livak, K.J. 2008. Analyzing real-time PCR data by the comparative C(T) method. *Nat Protoc* 3:1101-1108.

Publishing Agreement

It is the policy of the University to encourage the distribution of all theses, dissertations, and manuscripts. Copies of all UCSF theses, dissertations, and manuscripts will be routed to the library via the Graduate Division. The library will make all theses, dissertations, and manuscripts accessible to the public and will preserve these to the best of their abilities, in perpetuity.

Please sign the following statement:

I hereby grant permission to the Graduate Division of the University of California, San Francisco to release copies of my thesis, dissertation, or manuscript to the Campus Library to provide access and preservation, in whole or in part, in perpetuity.



Author Signature

6/29/12

Date